Accepted refereed manuscript of: Galindo A, Garrido D, Monroig O, Perez JA, Betancor M, Acosta NG, Kabeya N, Marrero M, Bolanos A & Rodriguez C (2021) Polyunsaturated fatty acid metabolism in three fish species with different trophic level. *Aquaculture*, 530, Art. No.: 735761. https://doi.org/10.1016/j.aquaculture.2020.735761

Polyunsaturated fatty acid metabolism in three fish species with different trophic level

A. Galindo[1], D. Garrido[1], Ó. Monroig[2], J.A. Pérez[1], M.B. Betancor[3], N.G. Acosta[1], N. Kabeya[4], M.A. Marrero[1], A. Bolaños[1], C. Rodríguez[1]

[1]Departamento de Biología Animal, Edafología y Geología, Universidad de La Laguna, Santa Cruz de Tenerife, Spain.

[2]Instituto de Acuicultura Torre de la Sal, Consejo Superior de Investigaciones Científicas (IATS-CSIC), 12595 Ribera de Cabanes, Castellón, Spain.

[3]Institute of Aquaculture, Faculty of Natural Sciences, University of Stirling, Stirling FK9 4LA, Scotland, United Kingdom.

[4]Department of Marine Biosciences, Tokyo University of Marine Science and Technology, 4-5-7 Konan, Minato-ku, Tokyo, Japan.

*Corresponding author: Covadonga Rodríguez

Mailing address: covarodr@ull.edu.es

Tel.: +34922316502 (Ext. 6574)

e-mail: covarodr@ull.edu.es

Abbreviations

ARA: arachidonic acid; BHT: butylated hydroxyl toluene; DHA: docosahexaenoic acid; dpm: desintegrations per minute; *ef1α*: elongation factor-1α; Elovl5: fatty acyl elongase 5; EPA: eicosapentaenoic acid; FA: fatty acid; Fads2: fatty acyl desaturase 2; FAF-BSA: fatty acid free bovine serum albumin; FAME: fatty acid methyl esters; FID: flame ionization detector; FO: fish oil; HBSS: Hanks balanced salt solution; LC-PUFA: long chain polyunsaturated fatty acid; NTC: negative controls; ORF: open reading fragment; PCR: polymerase chain reaction; PUFA: polyunsaturated fatty acid; qPCR: quantification real-time PCR; RACE: rapid amplification of cDNA ends; TL: total lipid; VO: vegetable oils**.**

Abstract

Reducing the dependency of fishfeed for marine ingredients and species diversification are both considered crucial factors for the sustainable development of aquaculture. The substitution of fish oil (FO) by vegetable oils (VO) in aquafeeds is an economically feasible solution. However, such substitution may compromise the fish flesh content of essential n-3 long chain polyunsaturated fatty acids (n-3 LC-PUFA) and, therefore, its nutritional value for human consumption. Likewise, there is a wide range of strategies to select new target species for sector diversification, among which, the capacity to biosynthesize n-3 LC-PUFA from their C_{18} precursors abundant in VO might be considered as a fair preliminary strategy. Therefore, the aim of the present study was to analyze the metabolic fate of [1-^{14}C] labeled 18:2n-6, 18:3n-3, 20:5n-3 and 22:6n-3 in isolated hepatocytes and enterocytes from wild individuals of three fish species with different trophic level: the marine herbivorous salema (*Sarpa salpa*), the strict carnivorous sand sole (*Pegusa lascaris*) and the omnivorous thicklip grey mullet (*Chelon labrosus*). These species were selected for their phylogenetic proximity to consolidated farmed species such as gilthead seabream (*Sparus aurata*), senegalese sole (*Solea senegalensis*), and golden grey mullet (*Liza aurata*), respectively. The study also assessed the molecular cloning, functional characterization and tissue distribution of the fatty acyl elongase (Elovl) gene, *elovl5*, involved in the biosynthetic metabolism of n-3 LC-PUFA. The three species were able to biosynthesize docosahexaenoic acid (22:6n-3). *S. salpa* seems to have similar biosynthetic capacity than *S. aurata*, with a fatty acyl desaturase 2 (Fads2), with Δ6, Δ8 and Δ5 activities. *P. lascaris* showed a wider Fads2 activity repertory than *S. senegalensis*, including Δ4 and residual Δ6/Δ5 activities. In *C. labrosus*, both Δ8 and Δ5 activities but not the Δ6 described for *L. aurata* were detected in the incubated cells. Elongation from C_{18} and C_{20} precursors to C_{20} and C_{22} products occurred

in hepatocytes and enterocytes as well as in the functional characterization of Elovl5 by heterologous expression in yeast. Elovl5 showed a species specific expression pattern, with the highest rates observed in the liver, gut and brain in *S. salpa* and *P. lascaris*, and in the brain for *C. labrosus*. In summary, the LC-PUFA biosynthesis capacity from *S. salpa*, *P. lascaris* and *C. labrosus* greatly resembled that of their phylogenetic closer species. The three studied species could be further explored as candidates for the aquaculture diversification from their potential ability to biosynthesize LC-PUFA.

Keywords

Chelon labrosus, Elovl5, LC-PUFA, *Pegusa lascaris, Sarpa salpa.*

1. Introduction

The annual per capita consumption of fish has risen up to 20.2 Kg in 2015, partly due to its contribution to the population needs for high-quality proteins, lipids and micronutrients (FAO, 2018). Lipids, and their main components, fatty acids (FA), are along with proteins, the largest organic components of fish. C_{18} polyunsaturated fatty acids (PUFA) such as 18:2n-6 and 18:3n-3, are considered essential nutrients for vertebrates because they cannot be synthesized *de novo*. Additionally, they are metabolic precursors of the physiologically important long-chain (C_{20-24}) PUFA (LC-PUFA) including arachidonic (20:4n-6, ARA), eicosapentaenoic (20:5n-3, EPA), and docosahexaenoic (22:6n-3, DHA) acids (Tocher, 2015). LC-PUFA are involved in key roles including cell membrane structure, transcription, regulation and cellular signalling (Lee et al., 2016; Tocher, 2015; Zárate et al., 2017). Particularly, the n-3 LC-PUFA 20:5n-3 and 22:6n-3 have been seen to prevent several human inflammatory and neurodegenerative illnesses (Lee et al., 2016; Zárate et al., 2017).

Fish, including farmed species, are the primary source of n-3 LC-PUFA for humans (Bell and Tocher, 2009). However, the fluctuating availability of marine ingredients used in aquafeed formulation, namely fish oil (FO) and fishmeal, their sustained price increase, the increment of global aquaculture production and the necessity to search for more sustainable alternatives to feed carnivorous species have resulted in a pressing need for their partial replacement by ingredients of terrestrial origin such as vegetable oils (VO). This practice reduces the n-3 LC-PUFA content in fish muscle (Pérez et al., 2014; Tocher, 2015) and therefore, its nutritional value to consumers. Recently, the use of oils from transgenic plants and the inclusion of micro and macroalgae-origin products rich in n-3 LC-PUFA have been proposed as possible novel alternatives to marine sources (Ruyter et al., 2019; Sprague et al., 2016; Tocher et al., 2019). Moreover, farming of fish species

with high capacity to biosynthesize LC-PUFA from their C_{18} precursors abundant in VO may also be considered as a valuable sustainable strategy for the aquaculture industry (Garrido et al., 2019). Therefore, it is essential to understand the LC-PUFA metabolism of potential candidate species for the diversification of aquaculture in order to select fish with high capacity to utilize dietary VO while maintaining proper growth and development, as well as its nutritional quality in terms of n-3 LC-PUFA content.

Liver is the main organ involved in lipid metabolism while gut have an important role in both uptake and LC-PUFA biosynthesis. In this sense, the incorporation and bioconversion of radiolabeled FA in enterocytes and hepatocytes from fish species have been demonstrated as an adequate tool to elucidate their LC-PUFA biosynthesis capabilities (Díaz-López et al., 2010; Garrido et al., 2020; Morais et al., 2015; Mourente and Tocher, 1993a, 1993b, 1994; Rodríguez et al., 2002; Tocher and Ghioni, 1999).

LC-PUFA biosynthesis in vertebrates including fish, is mediated by two types of enzymes (Monroig et al., 2018). On the one hand, the fatty acyl elongase (Elovl) proteins catalyze the condensation reaction of the fatty acid elongation pathway resulting in the extension of the fatty acyl chain in two carbons. Thus, enzymes such as Elovl5, Elovl2 and Elovl4 are being extensively studied in fish (Castro et al., 2016; Garlito et al., 2019; Monroig et al., 2018). On the other hand, fatty acyl desaturases (Fads) enzymes enter a double bond to PUFA substrates in between an existing one and the carbon of the carboxylic group. The Greek letter (Δ) is used to denote the position of the double bond created by Fads in the hydrocarbon chain. Unlike mammalian FADS2 that typically have Δ6/Δ8 activity (Castro et al., 2016), teleost Fads2 show high interspecific variability in their desaturase capacity. Thus, along with the Δ6/Δ8 activity (Monroig et al., 2011a), Fads2 with Δ4 and Δ5, as well as bifunctional Δ6/Δ5 desaturases have been reported (Castro et al., 2016; Garrido et al., 2020; Monroig et al., 2011a, 2018). The production of

20:4n-6 and 20:5n-3 from 18:2n-6 or 18:3n-3, respectively, may be obtained by a Δ6 desaturation activity towards C_{18} substrates followed by an elongation step and a final Δ5 desaturation (Fig. 1). Alternatively, a Δ8 desaturation over C_{20} intermediates may be also involved in the production of 20:4n-6 and 20:5n-3 from C_{18} precursors (Monroig et al., 2011a). The biosynthesis of 22:6n-3 from 20:5n-3 can be mediated via the Sprecher pathway (Sprecher, 2000), which requires two consecutive elongation steps, a Δ6 desaturation, and a final peroxisomal β-oxidation or through an alternative and more direct route with the action of a Δ4 desaturase (Li et al., 2010; Oboh et al., 2017) (Fig. 1).

The biosynthetic ability of each species to biosynthesize LC-PUFA was believed until very recently to depend on the species' habitat (freshwater *vs* marine), with marine species having limited capacity to convert C_{18} PUFA to LC-PUFA, and freshwater/diadromous fish having retained the ability to elongate and desaturate C_{18} precursors (Garrido et al., 2019; Monroig et al., 2018). Such generalization was questioned when the marine herbivore, *Siganus canaliculatus*, was reported to have a Δ4 Fads2 and a bifunctional Δ5/Δ6 Fads2 (Li et al., 2010). Further studies demonstrated the presence of Δ4 Fads2 in teleost species from a variety of habitats and trophic levels (Fonseca-Madrigal et al., 2014; Garrido et al., 2019; Kuah et al., 2015; Morais et al., 2012, 2015; Oboh et al., 2017). Thus, other factors such as phylogeny have been recently pointed out to influence the LC-PUFA biosynthetic capacity of teleosts (Castro et al., 2016; Garrido et al., 2019; Monroig et al., 2018). In teleosts, Elovl5 and Elovl2 share a common evolutionary origin (Monroig et al., 2016), and consequently, both of them have preference for C_{18} and C_{20} PUFA substrates although Elovl5 has also been reported to present some affinity towards C_{22} PUFA (Monroig et al., 2012).

In order to explore the potentiality of a wider range of species for the diversification of finfish aquaculture, based on their n-3 LC-PUFA biosynthesis capabilities, three fish

141 species with different trophic levels were selected in the present study: the salema *Sarpa*
142 *salpa* (Linnaeus, 1758), a marine herbivorous of the Sparidae family with trophic affinity
143 with *S. canaliculatus*; the sand sole *Pegusa lascaris* (Risso, 1810), a strict carnivorous
144 member of the Soleidae family that is phylogenetically close to *Solea senegalensis*; and
145 the thicklip grey mullet *Chelon labrosus* (Risso, 1827), a species from the Mugilidae
146 family closely related to *Liza aurata* with high adaptability to different feeding habits.
147 Molecular cloning, functional characterization and tissue distribution of Δ6 and Δ8
148 desaturase have been already described by our group in *S. salpa* and *C. labrosus*, as well
149 as Δ4 desaturase in *P. lascaris* (Garrido et al., 2019). However, their LC-PUFA
150 metabolism capacities were not completely characterized. To this aim, isolated
151 enterocytes and hepatocytes were incubated with different PUFA substrates, in order to
152 compare their uptake affinities and the ability of Fads2 and Elovl to desaturate and
153 elongate C_{18} and C_{20} radiolabeled FA precursors. Furthermore, the molecular cloning,
154 functional characterization and tissue distribution of *elovl5* elongases were also
155 elucidated. The results of the present study are discussed within the context of fish
156 nutrition and their applicability to the diversification of aquaculture with species able to
157 efficiently utilize ingredients alternative to FO.

2. Material and methods

2.1 Experimental animals and sampling

All experimental procedures were approved by the Ethical Committee at the University of La Laguna and were in accordance with the EU Directive 2010/63/EU regarding the protection and humane use of animals for scientific purpose (European Parliament and Council of the European Union, 2010).

Wild specimens of *S. salpa* (87.4 ± 14.4 g; n=5) and *C. labrosus* (12.5 ± 9.1 g; n=6) were captured by professional artisanal fishermen in Tenerife (Spain), while *P. lascaris* (111.2 ± 25.5 g; n=3) were captured off the coast of Huelva (Spain). Fish were subsequently transported to the laboratory for sacrifice and subsequent sampling. Samples of muscle, liver, heart, foregut, brain and gill were collected for molecular cloning, functional characterization and tissue distribution. Tissues were kept in RNAlater (Qiagen Iberia SL, Madrid, Spain) the first 24 h at 4ºC and then stored at -20ºC until analysis. In addition, the remaining foregut and liver were rapidly taken for the isolation of enterocytes and hepatocytes, respectively. The isolated cells were used for incubation and final extraction of the total lipid (TL) required to either assess the FA composition of control cells or to evaluate the incorporation of radioactivity into TL and the bioconversion rates of FA in the radiolabeled [1-^{14}C] incubated cells. Furthermore, muscle samples were also used for lipid and FA composition determination. The whole process was developed under an ice-cold environment to prevent sample degradation.

2.2 Isolation of enterocytes and hepatocytes and incubation with radiolabeled [1-^{14}C] fatty acids

Enterocytes and hepatocytes were obtained as described by Rodríguez et al. (2002). Organs from two or more fish were pooled in the case of *P. lascaris* and *C. labrosus* due to the small size of the animals. Before the beginning of the experiments, the foregut was

cleaned of food and feces and the liver perfused through the hepatic portal vein with a solution of marine Ringer containing 116 mM NaCl, 6 mM KCl, 1 mM $CaCl_2$, 1 mM $MgSO_4$, 10 mM $NaHCO_3$, 1 mM NaH_2PO_4, 10 mM K_2SO_4 and 10 mM HEPES (pH 7.4). Tissues were minced in Hanks balanced salt solution (HBSS) with NaCl 1.75% (w/v) (HBSS/NaCl), 9.69 mM HEPES, 1.73 mM $NaHCO_3$, and collagenase (10 mg/mL) and incubated with HBSS/collagenase in agitation for 40 min at 20ºC. The resultant cell suspensions were filtered through a 100 µm nylon mesh with HBSS including 1% (w/v) fatty acid free bovine serum albumin (FAF-BSA). Cells were collected by centrifugation (Beckman Coulter Allegra 25R, Indianapolis, USA) at 716 *g* for 10 min, washed with HBSS and re-centrifuged for 7 min. The isolated cells were then re-suspended in cold M199 medium with NaCl and a sample was taken to assess the viability of cells (over 90% in all cases) by using the trypan blue exclusion test.

Immediately after isolation, 6 mL of each cell preparation were incubated in sterile plastic flasks for 3 h with 40 µL (0.20 µCi) of radiolabeled [1-^{14}C] PUFA: 18:2n-6, 18:3n-3, 20:5n-3 or 22:6n-3, with specific activities of 124.3, 114.8, 122.1 and 122.1 dpm $pmol^{-1}$, respectively. A control incubation of 2 mL of each cell type suspension without the addition of radiolabeled FA was also performed under the same experimental conditions for the determination of FA profiles. Samples were stored at -80°C until analysis.

2.3 Lipid extraction and protein determination

The TL content of isolated cells (enterocytes and hepatocytes) was extracted after incubation with small modifications of the Folch method (Folch et al., 1957) as described by Christie and Han (2010). Briefly, either incubated control or radioactive cell preparations, were transferred into test tubes, centrifuged at 716 *g* for 5 min and the resultant pellets re-suspended in 4 mL of HBSS and re-centrifuged. Pellets were dissolved in 2 mL of 0.88% KCl (w/v), and 8 mL of chloroform/methanol (2:1, v/v) containing

0.01% (w/v) butylated hydroxytoluene (BHT) as antioxidant. After vigorous shaking, samples were re-centrifuged at 716 *g* for 5 min, the organic solvent collected, filtered, and evaporated under a stream of nitrogen. The TL content was determined gravimetrically, re-suspended in chloroform/methanol (2:1, v/v) with 0.01% (w/v) BHT and stored at -20ºC under an atmosphere of nitrogen until further analysis. For the lipid extraction of muscle samples, the same procedure as described above was performed, but tissue was previously homogenized in chloroform/methanol (2:1, v/v) using a Virtis rotor homogenizer (Virtishear, Virtis, Gardiner, New York).

Total protein content of incubated enterocytes and hepatocytes was determined in 100 µL-aliquots of cell suspensions, according to Lowry et al. (1951) using FAF-BSA as standard.

2.4 FA composition of non-radioactive samples

In order to assess the baseline FA composition of liver and gut epithelial cells from the three species, a smaller fraction (2 mL) of isolated enterocytes and hepatocytes suspensions that had been also incubated without [1-^{14}C] PUFA, were finally analyzed. Up to 1 mg of TL extracted from these control cell suspensions and from muscle samples were subjected to acid-catalyzed transmethylation to obtain fatty acid methyl esters (FAME). Resultant FAME were purified by thin-layer chromatography (Macherey-Nagel, Düren, Germany), separated and quantified using a TRACE-GC Ultra gas chromatograph (Thermo Scientific, Milan, Italy) equipped with an on-column injection, a flame ionization detector (FID) and a fused silica capillary column Supelcowax® 10 (30 m x 0.32 mm ID, df 0.25 µm) (Supelco Inc., Bellefonte, USA). Helium was used as the carrier gas at 1.5 mL/min constant flow, and temperature programming was from 50 to 150ºC at a rate of 40ºC/min, then from 150ºC to 200ºC at 2ºC/min, to 214ºC at 1ºC/min and, finally, to 230ºC at 40ºC/min, which was maintained for 3 min. Individual FAME

were identified by reference to authentic standards and further confirmation of FAME identity was carried out by GC-MS (DSQ II, Thermo Scientific) when necessary. The results are expressed as percentage of total FA.

Muscle FA composition of the three studied species is shown in the supplementary data table.

2.5 Metabolic fate of [1-^{14}C] PUFA. Incorporation of radioactivity into TL and bioconversion of radiolabeled FA

A 100 µg aliquot of TL from cells incubated with each radiolabeled FA (18:2n-6, 18:3n-3, 20:5n-3 or 22:6n-3) was used to determine the radioactivity incorporated by means of a liquid scintillation β-counter (TRI-CARB 4810TR, Perkin Elmer, Singapore). Results obtained in dpm were related to the specific activity of each fatty acid and to the cells TL and protein contents, and expressed as pmol mg prot^{-1} h^{-1}.

Desaturation-elongation capacities of isolated enterocytes and hepatocytes from the three fish species incubated with [1-^{14}C] PUFA (18:2n-6, 18:3n-3 and 20:5n-3) were determined using aliquots of up to 1 mg of the TL extract. Samples were subjected to acid-catalyzed transmethylation and the resultant FAME were then purified by argentation thin layer chromatography ($AgNO_3$-TLC) using TLC plates previously impregnated with 2 g silver nitrate in 20 mL acetonitrile and activated at 110ºC for 30 min. A known standard composed by a mixture of radiolabeled FA was also developed in the same plates for the identification of each band. TLC plates were fully developed in toluene/acetonitrile (95:5, v/v) to separate the bands of [1-^{14}C] FA (Wilson and Sargent, 1992). Then, they were placed in closed exposure cassettes in contact with a radioactive-sensitive phosphorous screen (Exposure Cassette-K, BioRad, Madrid, Spain) for two weeks. Screens were scanned with an image acquisition system (Molecular Imager Fx,

BioRad), and bands were identified and quantified in percentage of area using Quantity One 4.5.2. (BioRad) image software.

2.6 Molecular cloning of elovl5 cDNAs

Total RNA was extracted from each tissue (muscle, heart, liver, gut, brain and gill) and species using TRI Reagent (Sigma-Aldrich, Dorset, UK) following the manufacturer's instructions and using a bead tissue disruptor (Bio Spec, Bartlesville, Oklahoma, USA). Next, cDNA was synthesized from 2 μg of total RNA (mixture from brain and liver; 1:1) for each species using a High Capacity cDNA Reverse Transcription Kit (Applied Biosystems, California, USA) for molecular cloning. Subsequently, the first fragment of *elovl5* genes for each species were obtained by polymerase chain reaction (PCR) using the cDNA as template together with degenerated primers (Table 1) and GoTaq® Green Master Mix (Promega, Southampton, UK). The degenerated primers for *elovl5* were designed on conserved regions from sequences obtained from NCBI blastn tool (http://www.ncbi.nlm.nih.gov/) of several teleosts including *S. canaliculatus* (GU597350.1), *Epinephelus coioides* (KF006241.1), *Rachycentron canadum* (FJ440239.1), *S. senegalensis* (JN793448.1), *Chirostoma estor* (KJ417837.1), *S. aurata* (AY660879.1) and *Salmo salar* (NM_001123567.2). The alignment of *elovl5* sequences was carried out with BioEdit v7.0.9 (Tom Hall, Department of Microbiology, North Carolina State University, North Carolina, USA). The amplification of the first fragments by PCR were performed by an initial denaturing step at 95°C for 2 min, followed by the PCR conditions shown in Table 2 for each primer set, followed by a final extension at 72°C for 5 min. The amplified PCR fragments were purified on agarose gels using Illustra™ GFX™ PCR DNA and Gel Band Purification kit (GE Healthcare Life Sciences, Buckinghamshire, UK) and cloned into pGEM-T Easy vector (Promega) and sequenced (GATC Biotech, Konstanz, Germany). Then, the obtained sequences were used for

designing specific primers that allowed obtaining the 5' and 3' regions by Rapid Amplification of cDNA Ends (RACE). The cDNA for RACE was prepared by FirstChoice® RLM-RACE kit (Ambion, Applied Biosystems, Warrington, UK) following manufacturer's recommendations. All RACE PCR conditions and primers used are also reported in Tables 1 and 2. After the nested PCR using the first PCR product as a template, we successfully amplified each cDNA ends fragment. All RACE fragments were sequenced as described above and assembled with the corresponding first-fragments to obtain putative full-length cDNA.

2.7 Sequence and phylogenetic analyses

The deduced amino acid (aa) sequences of putative Elovl5 proteins isolated from *S. salpa*, *P. lascaris* and *C. labrosus* with a variety of functionally characterized Elovl2, Elovl4 and Elovl5 from vertebrates (human and fish) retrieved from NCBI were aligned using MAFFT (https://mafft.cbrc.jp/alignment/software/) Ver. 7.388 with the E-INS-i strategy (Katoh et al., 2019). All columns containing gaps in the obtained alignment were removed by trimAl (Capella-Gutiérrez et al., 2009). The cleaned alignment was subjected to a maximum likelihood phylogenetic analysis using RAxML with 1000 rapid bootstrap replicates. The best-fit evolutionary model was selected to LG+G+I for both genes by ModelTest-NG (Darriba et al., 2020). The resultant RAxML tree was visualized using Interactive Tree of Life v3 (Letunic and Bork, 2016).

2.8 Functional characterization

The open reading frames (ORF) of *elovl5* were amplified from *S. salpa*, *P. lascaris* and *C. labrosus* from liver cDNA by a nested PCR approach. All primers and PCR conditions are described in Tables 1 and 2. First-round of PCR used primer pairs designed for each species in the 5' and 3' untranslated regions (UTR) for forward and reverse

306 primers, respectively. Second round of PCR was run using the first-round PCR products
307 as templates and primers containing restriction sites (underlined in Table 1) for
308 subsequent ligation into the yeast expression vector pYES2 (Thermo Fisher Scientific,
309 Hemel Hempstead, UK). In the case of *P. lascaris,* both first and second round PCR were
310 performed with the high fidelity *Pfu* DNA polymerase (Promega), whereas for *S. salpa*
311 and *C. labrosus elovl5* the PfuUltra II Fusion HS DNA Polymerase (Agilent, Santa Clara,
312 California, USA) was used. Subsequently, the PCR products were purified, digested with
313 the corresponding restriction enzymes (New England BioLabs, Hitchin, UK) and ligated
314 into a similarly restricted pYES2. The plasmids containing pYES2-*elovl5* from each
315 species were purified (GenElute™ Plasmid Miniprep Kit, Sigma) and sequenced before
316 being transformed into yeast *Saccharomyces cerevisiae* competent cells InvSc1 (Thermo
317 Fisher Scientific). Transformation and selection of yeast culture were performed as
318 described by Garrido et al. (2019). One single yeast colony transformed with pYES2-
319 *elovl5* for each species was used for functional assays. The transgenic yeasts were grown
320 in the presence of one of the potential FA substrates for elongases, namely 18:2n-6, 18:3n-
321 3, 18:3n-6, 18:4n-3, 20:4n-6, 20:5n-3, 22:4n-6 and 22:5n-3. The FA substrates were
322 added to the yeast cultures at final concentrations of 0.5 mM (C_{18}), 0.75 mM (C_{20}) and
323 1.0 mM (C_{22}) as uptake efficiency decreases with increasing chain length (Kabeya et al.,
324 2018). In addition, yeasts transformed with empty pYES2 were also grown in the presence
325 of each substrate as control treatments. After 2 days of culture at 30°C, yeasts were
326 harvested, washed, and TL extracted by homogenization in chloroform/methanol (2:1,
327 v/v) containing 0.01% (w/v) BHT as antioxidant.

328 **2.9 Fatty acid analysis of yeast**

329 FAME were determined from the TL extracted from yeast according to Hastings et al.
330 (2001). FAME were separated and quantified using a Fisons GC-8160 (Thermo Fisher

Scientific) gas chromatograph equipped with a 60 m x 0.32 mm i.d. x 0.25 μm ZB-wax column (Phenomenex, Macclesfield, UK) and flame ionization detector. The elongation conversion efficiencies from exogenously added PUFA substrates were calculated by the proportion of substrate FA converted to elongated products as [product area / (product area + substrate area)] × 100.

2.10 Tissue expression of *elovl5*

Expression of the *elovl5* gene was determined by quantitative real-time PCR (qPCR) in muscle, heart, liver, gut, brain and gill, being the number of replicates n=4 in *S. salpa* and *P. lascaris*, and n=3 in *C. labrosus*. Elongation factor-1α (*ef1α*) and β-actin (*actb*) and 18S were tested as potential reference genes for normalization of *elovl5* expression, with *ef1α* and *actb* being selected for that purpose since they were the most stable genes according to geNorm (M stability value = 0.165; Vandesompele et al., 2002). Total RNA was extracted and 2 μg of each sample were reverse transcribed into cDNA as described above. In the interest of assessing the efficiency of the primer pairs, serial dilutions of pooled cDNA were carried out for each species. All qPCR were performed by a Biometra TOptical Thermocycler (Analytik Jena, Jena, Germany) in 96-well plates in duplicates at total volume of 20 μL containing 10 μL of Luminaris Color HiGreen qPCR Master Mix (Thermo Fisher Scientific), 1 μL of each primer (10 μM), 2 μL or 5 μL of cDNA (1/20 dilutions) for reference and target genes, respectively, as well as 6 or 3 μL of molecular biology grade water. Besides, negative controls (NTC, no template control), containing molecular biology grade water instead of cDNA, were also run in each plate. The primer sequences and qPCR conditions are detailed in Tables 1 and 2, respectively. The relative expression of *elovl5* among tissues in each species was calculated as arbitrary units after normalization dividing by the geometric mean of the expression level of the reference genes *elf1α* and *actb*. One arbitrary unit is defined as the ratio between the expression

level of *elovl5* and the lowest expression level for this gene. After each qPCR analysis, a melting curve with 1°C increments during 6 s from 60 to 95°C was performed, in order to check the presence of a single product in each reaction.

2.11 Statistical analysis

Results for TL, FA composition, incorporation of radioactivity into TL, and bioconversions of enterocytes and hepatocytes incubated with [1-^{14}C] FA substrates are presented as mean ± SD (n=5 for *S. salpa*, except for [1-^{14}C] 22:6n-3 where n=4; n=6 for *C. labrosus* and n=3 for *P. lascaris*). Tissue expression is presented as log 10 mean normalized ratios ± standard error (N). *P* values of less than 0.05 were considered significantly different for all statistical test applied. Normal distribution of the data and homogeneity of the variances were verified with the one-sample Shapiro-Wilk test and the Levene test, respectively (Zar, 1999).

Statistical differences in the incorporation of radioactivity into TL in enterocytes and hepatocytes incubated with [1-^{14}C]FA substrates (18:2n-6, 18:3n-3, 20:5n-3 and 22:6n-3), the bioconversions of [1-^{14}C]FA substrates in enterocytes and hepatocytes (18:2n-6, 18:3n-3 and 20:5n-3) as well as tissue expression were tested by one-way ANOVA followed by a Tukey HSD multiple comparison test (Zar, 1999) for each cell type and species. When homocedasticity was not achieved, data were transformed using logarithm or arcsine square root. If transformations did not succeed, Welch test was performed, followed by T3 Dunnet. Kruskall-Wallis non-parametric test was applied in the case of no normal distribution followed by pair-wise comparisons Mann-Whitney test with Bonferroni correction. When one group was missing, the remaining two groups were analyzed by t-student or Mann-Whitney tests for no normal data. All statistical analyses were performed using the IBM SPSS statistics 25.0 for Windows (SPSS Inc., New York, USA).

3. Results

3.1 Lipid content and fatty acid composition of control cells, and incorporation of radioactivity into total lipids of cells incubated with [1-^{14}C] radiolabeled FA

Table 3 shows the FA composition of enterocytes and hepatocytes from the three fish species studied. Saturates, mainly represented by 16:0, was the most abundant group of FA (29.3-50.4%) in both cell types in all the species. Monounsaturated FA ranged between 13.7 and 28.9% of total FA, with about two-thirds being 18:1n-9. In enterocytes, total monounsaturated was slightly higher in *P. lascaris* (24.6% *vs* 13.7-16.3%). N-3 PUFA were an important group of FA in this cell type, remaining fairly stable among species (23.7-26.7%). 20:4n-6 and 20:5n-3 were more abundant in *S. salpa* (~15%) than in *P. lascaris* and *C. labrosus* (ranging between 2.5 and 5.9%) whereas 22:6n-3 was more relevant in *P. lascaris* (16.0 ± 5.0%) and *C. labrosus* (18.4 ± 4.9%) than in *S. salpa* (2.8 ± 0.3%). Finally, 18:2n-6 represented between 3.5 and 7.7% of total FA in enterocytes from the three species. The FA composition of hepatocytes from *S. salpa* showed higher proportions of total n-3 PUFA, 20:5n-3, 22:5n-3 and 20:4n-6 than *P. lascaris* and *C. labrosus* while 22:6n-3 content was higher in hepatocytes from *C. labrosus* (12.3%) in comparison to *S. salpa* and *P. lascaris* (5.1% and 5.2%, respectively) (Table 3).

Table 4 shows the incorporation of radioactivity into TL of enterocytes and hepatocytes of the three species. Overall, both [1-^{14}C] C_{18} PUFA were generally the most incorporated FA in both cell types. Regardless of cell type and fish species, [1-^{14}C] 22:6n-3 tended to be the least incorporated FA. *P. lascaris* presented the highest values of incorporation for all radiolabeled substrates in enterocytes, and for [1-^{14}C] 18:3n-3 in hepatocytes. FA incorporation seems to be higher in hepatocytes than in enterocytes of *S. salpa*. By contrast, *P. lascaris* presented the opposite trend although [1-^{14}C] 22:6n-3 did not differ between isolated cells (Table 4).

406 **3.2 Bioconversion of radiolabeled FAs**

407 Bioconversion of [1-^{14}C] 18:2n-6, 18:3n-3 and 20:5n-3 in enterocytes and hepatocytes
408 of the three fish species studied is shown in Table 5. Regardless of cellular type and
409 species, the majority of radioactivity was consistently recovered as the unmodified
410 substrate (59.1-92.3%). Nonetheless, enterocytes tended to show higher bioconversion
411 rates (estimated as the sum of the products derived from each radiolabeled substrate) in
412 both *S. salpa* (ranging from 10.6 to 37.0%) and *C. labrosus* (ranging from 10.3 to 37.6%)
413 than in *P. lascaris* (ranging from 7.7 to 29.3%), with [1-^{14}C] 20:5n-3 being the most
414 modified FA (29.3-37.6%) in the three species (Table 5). Elongation was the most
415 prominent activity over all substrates assayed in enterocytes from both *S. salpa* and *P.*
416 *lascaris* and only over 20:5n-3 in *C. labrosus*. In addition, desaturation was registered
417 exclusively towards [1-^{14}C] 18:3n-3 in *S. salpa* and [1-^{14}C] 18:2n-6 in *P. lascaris* (<1%).
418 On the other hand, products obtained from the action of both elongases and desaturases
419 (E+D, elongation/desaturation) over the radiolabeled PUFA notably varied among
420 substrates and species in this cellular type. Thus, E+D products from [1-^{14}C] 20:5n-3 were
421 significantly more abundant than those from [1-^{14}C] 18:3n-3 in *S. salpa*, whereas [1-^{14}C]
422 18:2n-6 was the most modified substrate in *C. labrosus* (Table 5).

423 [1-^{14}C] 20:5n-3 was also the most modified PUFA (22.5-40.9%) in hepatocytes except
424 in *C. labrosus*, where [1-^{14}C] 18:2n-6 was bio-converted to a similar extent (Table 5).
425 Similarly to enterocytes, elongation was the most common activity over all substrates in
426 hepatocytes from *P. lascaris* and *S. salpa* (8.1-32.1% and 8.7-17.4%, respectively), and
427 additionally, over [1-^{14}C] 20:5n-3 in *C. labrosus* (21.9 ± 3.4%). Desaturation was
428 exclusively observed towards both [1-^{14}C] C_{18} PUFA in *S. salpa* and towards [1-^{14}C]
429 18:2n-6 in *P. lascaris*, being in all cases < 3%. Moreover, E+D activity varied from 1.9
430 to 22.2% between substrates and species (Table 5). Thus, [1-^{14}C] 18:2n-6 tended to be

the most elongated and desaturated FA in hepatocytes from all species although only at a significant rate in *S. salpa.*

Desaturation over [1-^{14}C] 18:3n-3 and [1-^{14}C] 18:2n-6 in enterocytes from *S. salpa* and *P. lascaris*, respectively, led to the production of 18:4n-3 (0.3 ± 0.4%) and 18:3n-6 (1.0 ± 0.7%), respectively (Table 6). Although transformation of [1-^{14}C] 18:2n-6 to 20:4n-6 was only present in *C. labrosus* (1.3 ± 0.4%), 22:5n-6 was detected in all species (Table 6). With respect to the n-3 series, both 20:5n-3 and 22:6n-3 were obtained from [1-^{14}C] 18:3n-3 in *P. lascaris* (0.3 ± 0.2 and 0.5 ± 0.5%, respectively) and *C. labrosus* (0.8 ± 0.3 and 1.2 ± 0.3%, respectively) but not in *S. salpa*. However, only *P. lascaris* was able to synthesize 22:6n-3 from [1-^{14}C] 20:5n-3 (4.6 ± 5.9%) (Table 6).

Furthermore, 20:4n-6 was produced from [1-^{14}C] 18:2n-6 in hepatocytes from both *S. salpa* (0.4 ± 0.5%) and *C. labrosus* (9.9 ± 6.7%). In addition, [1-^{14}C] 18:3n-3 was bioconverted in a similar pattern as described above for enterocytes. More specifically, both 20:5n-3 and 22:6n-3 were obtained from [1-^{14}C] 18:3n-3 in *P. lascaris* (1.2 ± 0.4% and 0.4 ± 0.7%, respectively) and *C. labrosus* (0.8 ± 0.7 and 1.4 ± 1.2%, respectively), whereas only 22:6n-3 was detected in *S. salpa* (0.9 ± 0.3%). Besides, only *P. lascaris* synthesize 22:6n-3 from [1-^{14}C] 20:5n-3 (Table 6).

3.3 Elovl5 sequences, phylogenetics, functional characterization and tissue expression

Elovl5 elongase from *S. salpa*, *P. lascaris* and *C. labrosus* consist of an ORF of 885, 867 and 876 bp, encoding putative proteins of 295, 289 and 292 aa, respectively. The newly cloned *elovl5* cDNA sequences were deposited in the GenBank database under the accession numbers MT019561, MT019562 and MT019563. Our phylogenetic analysis showed that the three elongases clustered together within a branch containing Elovl5 from

455 vertebrates, itself separated from other PUFA elongases, namely Elovl2 and Elovl4 (Fig.
456 2). These results confirm that the sequences investigated herein are all Elovl5 elongases.
457 The putative proteins encoded by the *elovl5* cDNA sequences were functionally
458 characterized in yeast. Our results show that the three Elovl5 had activity over all C_{18} and
459 C_{20} PUFA substrates assayed (Table 7). With the exception of Elovl5 in *P. lascaris* which
460 exhibited a remarkably low activity towards 22:5n-3, the herein functionally
461 characterized Elovl5 did not have the capacity to elongate C_{22} PUFA substrates (Table
462 7).
463 The highest expression of *elovl5* in both *S. salpa* and *P. lascaris* was observed in liver,
464 gut and brain whereas in *C. labrosus*, brain presented the highest expression ratio, and
465 liver and gill the lowest ones (Fig. 3).
466

4. Discussion

The ability of fish to biosynthesize LC-PUFA is one of the factors to be considered to determine the potential interest of a particular species as candidate for the diversification of aquaculture. Thus, it could allow for both the development of feedstuff formulations optimized for the target species as well as the selection of fish with high capacity to utilize C_{18} fatty acid precursors from dietary VO while maintaining proper growth and development, and its nutritional quality in terms of flesh n-3 LC-PUFA content.

In the present work, the incorporation of radioactivity into total lipids of isolated cells from the three fish species studied (*S. salpa*, *P. lascaris* and *C. labrosus*) showed notable differences between [1-^{14}C] C_{18} PUFA precursors (18:2n-6 and 18:3n-3) and [1-^{14}C] LC-PUFA (20:5n-3 and 22:6n-3). Overall, both enterocytes and hepatocytes seem to preferentially incorporate C_{18} precursors, followed by 20:5n-3 and finally 22:6n-3 (Table 4), in spite of the reported physiological importance of these two LC-PUFA. A similar pattern was found in juvenile of *S. aurata* (Mourente and Tocher, 1993a). However, due to results obtained in a subsequent study in *S. aurata*, together with studies in *L. aurata* and *Scophthalmus maximus* (Linares and Henderson, 1991; Mourente and Tocher, 1993b, 1994), a preferential retention of 20:5n-3 in marine fish was proposed (Mourente and Tocher, 1994). A lower affinity of proteins involved in FA membrane translocation processes for LC-PUFA and a poorer ability of $\geq C_{20}$ PUFA to diffuse through cell membranes (Pérez et al., 1999) may be responsible for the observed incorporation differences. In addition, although β-oxidation measurement was not carried out in our study due to sample limitation, a preferential β-oxidation activity over C_{18} precursors could not be ruled out since C_{18} PUFA are readily oxidized substrates, in comparison with LC-PUFA, which are mostly preserved and stored in tissue membranes (Almaida-Pagán et al., 2007; Mourente et al., 2005). Thus, the apparent affinity for C_{18} PUFA in the

492 studied species may be due either, to the ability of cells to more easily incorporate FA
493 with shorter chains (C_{18} *vs.* $\geq C_{20\text{-}22}$) or to their preference to be β-oxidized.

494 Regardless of the species, bioconversion rates in enterocytes and hepatocytes ranged
495 between 7.7 and 40.9% (Table 5), showing higher bioconversion capacities than other
496 teleosts previously studied such as *S. aurata*, *S. maximus* or *S. senegalensis* (Díaz-López
497 et al., 2010; Morais et al., 2015; Rodríguez et al., 2002). Moreover, as it has been
498 previously reported in *S. maximus* and *S. senegalensis* (Morais et al., 2015; Rodríguez et
499 al., 2002), 20:5n-3 is the most modified FA, mainly elongated by Elovl5 action, in the
500 enterocytes of the three species, and in the hepatocytes of *S. salpa* and *P. lascaris*. In spite
501 of this, 22:6n-3 from [1-^{14}C] 20:5n-3 was only detected in *P. lascaris* (Table 6), probably
502 due to the Δ4 activity described before (Garrido et al., 2019), although the Sprecher route
503 may not be completely ruled out in this species, as it will be further discussed in this work.

504 Our recent previous results (Garrido et al., 2019) demonstrated the existence of a Fads2
505 with Δ6 and Δ8 activities in *S. salpa* by heterologous expression in yeast. Therefore, the
506 presence of 18:4n-3 and 24:6n-3 in both enterocytes and hepatocytes of *S. salpa* incubated
507 with [1-^{14}C] 18:3n-3 agrees well with the Δ6 activity above mentioned, although for
508 incubations with [1-^{14}C] 18:2n-6 this activity was found exclusively in hepatocytes (Table
509 6). Also in agreement with our results on *S. salpa*, the Δ6 activity for Fads2 towards both
510 18:3n-3 and 24:5n-3 has also been observed in *S. aurata* using radioactivity-based assays
511 and yeast expression systems (Mourente and Tocher, 1993a; Oboh et al., 2017; Tocher
512 and Ghioni, 1999). Moreover, as reported herein for *S. salpa*, 18:3n-6 but not 24:5n-6
513 was detected in *S. aurata in vivo* assays or when fibroblasts were incubated with [1-^{14}C]
514 18:2n-6 (Mourente and Tocher, 1993a; Tocher and Ghioni, 1999). Our present results in
515 *S. salpa* add more evidences to the possible conservation of the Δ6 desaturase capacity
516 among members of the Sparidae family as previously reported in *S. aurata*. In addition,

517 the presence of 20:3n-6 and 20:4n-3 in hepatocytes (Table 6), confirms the Δ8 activity
518 recently suggested by our results using molecular tools (Garrido et al., 2019). A Δ5
519 desaturation activity was also detected in hepatocytes of *S. salpa*, obtaining 20:4n-6 from
520 the incubation with [1-^{14}C] 18:2n-6. Activities, which have been also reported in *S.*
521 *aurata*, together with the presence of trace levels of 20:5n-3. Thus, it is possible that
522 Fads2 had also some Δ6/Δ5 activity in these sparids. Finally, 22:6n-3 was only detected
523 in hepatocytes incubated with [1-^{14}C] 18:3n-3 but not with [1-^{14}C] 20:5n-3. The lower
524 total incorporation of [1-^{14}C] 20:5n-3 compared to [1-^{14}C] 18:3n-3 in *S. salpa*, may
525 explain these differences of bioconversion rates between substrates.

526 *S. salpa* displayed elongation activity in both the radiolabeled assays and in the
527 functional characterization of Elovl5 by heterologous expression in yeast, obtaining C_{20}
528 and C_{22} products from the C_{18} and C_{20} precursors, respectively (Table 6, 7). Elovl5 is
529 known to mainly act over C_{18} and C_{20} substrates as indicated by heterologous expression
530 in yeast (Monroig et al., 2012). Furthermore, elongation activity over C_{22} PUFA was also
531 observed in our study when cells were incubated with [1-^{14}C] 20:5n-3 according to what
532 has been reported in *S. aurata* (Agaba et al., 2005). Collectively, our results indicate that
533 both *S. salpa* and *S. aurata* have a rather similar capacity for LC-PUFA biosynthesis
534 despite the remarkably different trophic level of these two sparid species.

535 *P. lascaris* enterocytes and hepatocytes displayed similar lipid metabolic
536 characteristics. C_{20}, C_{22} and C_{24} FAs were detected as elongation products when both cell
537 types were incubated in the presence of [1-^{14}C] C_{18} and [1-^{14}C] C_{20} substrates, in
538 accordance to the Elovl5 activities detected in yeast (Table 6, 7), and as reported by
539 Morais et al. (2012) in its phylogenetically close *S. senegalensis*. At the same time,
540 multiple products of desaturation were identified with our experimental design. On one
541 hand, the presence of 22:5n-6 from [1-^{14}C] 18:2n-6 as well as that of 22:6n-3 when

incubating with [1-^{14}C] 18:3n-3 and [1-^{14}C] 20:5n-3 (Fig. 1) in both cell types could confirm the Δ4 activity previously reported by our group with a molecular approach (Garrido et al., 2019). Nevertheless, these results seem to indicate that this species could have another Fads2 with Δ6/Δ5 activity still uncharacterized. On the other hand, our radioactive assays suggest the existence of Δ6 and Δ8 activities when incubating with [1-^{14}C] 18:2n-6, based on the detection of 18:3n-6 and 20:3n-6, as well as 24:5n-6 in enterocytes (Table 6). While similar bioconversions were not registered when using [1-^{14}C] 18:3n-3 as substrate, the transformations towards [1-^{14}C] 18:2n-6 indicate that *P. lascaris* may possess, along with the Δ4 Fads2 previously alluded (Garrido et al., 2019), a second Fads2 with Δ6/Δ8 activities, and a possible residual Δ6/Δ5 activity as Morais et al. (2015) suggested in *S. senegalensis*. What is more, perhaps a n-6 preference/specificity could be the reason why Morais et al. (2015) did not find Δ6 activity in *S. senegalensis*, since only [1-^{14}C] 18:3n-3 and [1-^{14}C] 20:5n-3 were used as substrates. Importantly, these results suggest that *P. lascaris* seems to be able to biosynthesize 22:6n-3 via two different routes, namely the Δ4 pathway operated by the functionally characterized Fads2 (Garrido et al., 2019), and the Sprecher pathway operated by a yet uncharacterized Fads2.

The enzymatic activity assays carried out on *C. labrosus* enterocytes and hepatocytes demonstrated that this species has Δ8 and Δ5 desaturase capacities, as well as the ability to biosynthesize 22:6n-3 from [1-^{14}C] 18:3n-3 (Table 6). Although the Δ8 desaturase activity was demonstrated in the Δ6/Δ8 Fads2 characterized in our earlier study on *C. labrosus* (Garrido et al., 2019), no activity as Δ5 desaturase was detected through molecular tools for that enzyme. Therefore, the present study performed in isolated cells suggest that *C. labrosus* has extra copies of Fads2, possibly containing Δ5 desaturation capacity. Consequently, the coexistence of Δ5, Δ6 and Δ8 activities within *C. labrosus* may account for all the desaturation reactions required for the bioconversion of 18:3n-3

567 to 22:6n-3 detected in our experiments. 22:6n-3 biosynthesis seemed to be performed by
568 the Sprecher pathway as it has been previously described for *L. aurata* (Mourente and
569 Tocher, 1993b). However, as C_{24} intermediaries of the Sprecher pathway were not
570 detected in the enzymatic assays (Table 6), the Δ4 pathway cannot be completely ruled
571 out. Fads2 with Δ4 activity has not been yet characterized in the Mugilidae family, but it
572 has been demonstrated in other families from the same lineage Ovalentaria, such as
573 Cichlidae or Atherinidae (Fonseca-Madrigal et al., 2014; Garrido et al., 2019; Oboh et
574 al., 2017). 22:6n-3 is biosynthesized from [1-^{14}C] 18:3n-3 but not from [1-^{14}C] 20:5n-3
575 in *C. labrosus*. In *S. salar*, the addition of 20:5n-3 inhibited LC-PUFA biosynthesis in
576 cells lines (AS) (Zheng et al., 2009b), while increasing doses of 20:5n-3 decreased the Δ5
577 and Δ6 gene expression in the same species Kjær et al. (2016). This, together with the
578 lower incorporation into total lipid of [1-^{14}C] 20:5n-3 *vs*. [1-^{14}C] 18:3n-3, could account
579 for the differences found between both substrates (Table 4).

580 Both the functional characterization of Elovl5 in yeast and radiolabeled assays with
581 isolated cells showed elongation from C_{18} and C_{20} precursors to C_{20} and C_{22} products
582 (Table 6, 7), respectively, in *C. labrosus*. The detection of 24:5n-3 when both cell types
583 were incubated with [1-^{14}C] 20:5n-3 could indicate the action of other Elovl, such as
584 Elovl4, which is able to elongate a range of PUFA substrates including 22:5n-3 (Monroig
585 et al., 2011b, 2012).

586 The gene expression pattern of *elovl5* varied among species. *S. salpa* and *P. lascaris*
587 had the highest number of transcripts in the liver, gut and brain, while this occurred in the
588 brain of *C. labrosus*, where liver and gill showed the lowest expression (Fig. 3). Until
589 now, the differences in tissue gene expression distribution have been hypothesized to be
590 associated to the origin of the species (marine or freshwater) (Kabeya et al., 2017).
591 Furthermore, it is known that different factors such as nutritional history, developmental

592 stage, etc., can affect the tissue distribution patterns of *elovl5* (Monroig et al., 2018).
593 Besides gut and liver, a few evidences suggest that other tissues can also biosynthesize
594 LC-PUFA. In this sense, the brain is a conservative tissue rich in LC-PUFA and therefore,
595 a higher number of transcripts could be necessary in order to satisfy an optimal level of
596 LC-PUFA for proper function (Zheng et al., 2009a).

597 It has been hypothesized that fish occupying low trophic levels, require only C_{18} PUFA
598 in the diet, being capable of *de novo* biosynthesize LC-PUFA, while those with high
599 trophic levels, are unable to form LC-PUFA from C_{18} precursors and therefore need a
600 dietary supply of LC-PUFA. Nonetheless, fish occupying intermediate trophic level,
601 which may require either C_{18} PUFA or LC-PUFA depending on their ecological niche
602 and life history, called into question this generalization (Trushenski and Rombenso,
603 2019). Our results obtained in three fish species with different trophic level, indicate that
604 this factor might not be a good indicator for LC-PUFA biosynthesis.

605 In conclusion, phylogeny of the fish species, instead of trophic level, might be a more
606 relevant factor in the LC-PUFA biosynthetic capacity. *S. salpa* and *P. lascaris* showed
607 lipid metabolism characteristics similar to two established commercial species such as *S.*
608 *aurata* and *S. senegalensis*, respectively, and could be adequate candidates for
609 aquaculture diversification. The LC-PUFA biosynthetic capacity of wild *S. salpa*, *P.*
610 *lascaris* and *C. labrosus* resembled that of their phylogenetically close species *S. aurata*,
611 *S. senegalensis* and *L. aurata*, respectively. The desaturase activities observed in this
612 study include Δ5, Δ6 and Δ8 activities in *S. salpa*, Δ5 and Δ8 activity in *C. labrosus*, and
613 Δ6/Δ5 residual activity and Δ4 in *P. lascaris*. Thus, confirming the ability of the three
614 species studied to biosynthesize 22:6n-3 from 18:3n-3.
615

Acknowledgments

This study was funded by Ministerio de Economía y Competitividad (AGL2015-70994-R). A. Galindo and M. Marrero are supported by a PhD grant by Cajasiete and Gobierno de Canarias, respectively. Dr. Covadonga Rodríguez and Dr. Ana Bolaños are members of the Instituto de Tecnologías Biomédicas de Canarias (ITB). We also thank Dr. Inmaculada Giráldez from Universidad de Huelva for her assistance with laboratory facilities and Dr. Deiene Rodríguez-Barreto for her useful revision and assistance with the manuscript.

References

Agaba, M.K., Tocher, D.R., Zheng, X., Dickson, C.A., Dick, J.R., Teale, A.J., 2005. Cloning and functional characterisation of polyunsaturated fatty acid elongases of marine and freshwater teleost fish. Comp. Biochem. Physiol. Part B Biochem. Mol. Biol. 142, 342-352.

Almaida-Pagán, P.F., Hernández, M.D., García García, B., Madrid, J.A., De Costa, J., Mendiola, P., 2007. Effects of total replacement of fish oil by vegetable oils on n-3 and n-6 polyunsaturated fatty acid desaturation and elongation in sharpsnout seabream (*Diplodus puntazzo*) hepatocytes and enterocytes. Aquaculture 272, 589-598.

Bell, M. V, Tocher, D.R., 2009. Biosynthesis of polyunsaturated fatty acids in aquatic ecosystems: general pathways and new directions, in: Kainz, M., Brett, M.T., Arts, M.T. (Eds.), Lipids in Aquatic Ecosystems. Springer New York, New York, NY, pp. 211-236.

Capella-Gutiérrez, S., Silla-Martínez, J.M., Gabaldón, T., 2009. trimAl: a tool for automated alignment trimming in large-scale phylogenetic analyses. Bioinformatics 25, 1972-1973.

Castro, L.F.C., Tocher, D.R., Monroig, Ó., 2016. Long-chain polyunsaturated fatty acid biosynthesis in chordates: Insights into the evolution of Fads and Elovl gene repertoire. Prog. Lipid Res. 62, 25-40.

Christie, W.W., Han, X., 2010. Lipid analysis: isolation, separation, identification and lipidomic analysis. Oily Press, an imprint of PJ Barnes & Associates, pp. 55-66.

Darriba, D., Posada, D., Kozlov, A.M., Stamatakis, A., Morel, B., Flouri, T., 2020. ModelTest-NG: a new and scalable tool for the selection of DNA and protein

evolutionary models. Mol. Biol. Evol. 37, 291-294.

Díaz-López, M., Pérez, M.J., Acosta, N.G., Jerez, S., Dorta-Guerra, R., Tocher, D.R., Lorenzo, A., Rodríguez, C., 2010. Effects of dietary fish oil substitution by Echium oil on enterocyte and hepatocyte lipid metabolism of gilthead seabream (*Sparus aurata* L.). Comp. Biochem. Physiol. Part B Biochem. Mol. Biol. 155, 371-379.

FAO, 2018. The state of world fisheries and aquaculture 2018: Meeting the sustainable development goals. Rome. Licence: CC BY-NC-SA 3.0 IGO.

Folch, J., Lees, M., Sloane-Stanley, G.H., 1957. A Simple method for the isolation and purification of total lipides from animal tissues. J. Biol. Chem. 226, 497-509.

Fonseca-Madrigal, J., Navarro, J.C., Hontoria, F., Tocher, D.R., Martínez-Palacios, C.A., Monroig, Ó., 2014. Diversification of substrate specificities in teleostei Fads2: characterization of Δ4 and Δ6Δ5 desaturases of *Chirostoma estor*. J. Lipid Res. 55, 1408-1419.

Garlito, B., Portoles, T., Niessen, W.M.A., Navarro, J.C., Hontoria, F., Monroig. Ó., Varó, I., Serrano, R., 2019. Identification of very long-chain (>C24) fatty acid methyl esters using gas chromatography coupled to quadrupole/time-of-flight mass spectrometry with atmospheric pressure chemical ionization source. Anal. Chim. Acta 1051, 103-109.

Garrido, D., Kabeya, N., Betancor, M.B., Pérez, J.A., Acosta, N.G., Tocher, D.R., Rodríguez, C., Monroig, Ó., 2019. Functional diversification of teleost Fads2 fatty acyl desaturases occurs independently of the trophic level. Sci. Rep. 9, 11199.

Garrido, D., Monroig, O., Galindo, A., Betancor, M. B., Perez, J. A., Kabeya, N., Marrero, M., Rodríguez, C. 2020. Lipid metabolism in *Tinca tinca* and its n-3 LC-PUFA biosynthesis capacity. Aquaculture, 523, 735147.

672 Hastings, N., Agaba, M., Tocher, D.R., Leaver, M.J., Dick, J.R., Sargent, J.R., Teale,
673 A.J., 2001. A vertebrate fatty acid desaturase with Delta 5 and Delta 6 activities.
674 Proc. Natl. Acad. Sci. U. S. A. 98, 14304-14309.

675 Kabeya, N., Chiba, M., Haga, Y., Satoh, S., Yoshizaki, G. 2017. Cloning and functional
676 characterization of fads2 desaturase and elovl5 elongase from Japanese flounder
677 *Paralichthys olivaceus*. Comp. Biochem. Physiol. Part B Biochem. Mol. Biol. 214,
678 36-46.

679 Kabeya, N., Yevzelman, S., Oboh, A., Tocher, D.R., Monroig, Ó., 2018. Essential fatty
680 acid metabolism and requirements of the cleaner fish, ballan wrasse *Labrus bergylta*:
681 Defining pathways of long-chain polyunsaturated fatty acid biosynthesis.
682 Aquaculture 488, 199-206.

683 Katoh, K., Rozewicki, J., Yamada, K.D., 2019. MAFFT online service: multiple sequence
684 alignment, interactive sequence choice and visualization. Brief. Bioinform. 20,
685 1160-1166.

686 Kjær, M.A., Ruyter, B., Berge, G.M., Sun, Y., Østbye, T.-K.K., 2016. Regulation of the
687 omega-3 fatty acid biosynthetic pathway in Atlantic salmon hepatocytes. PLoS One
688 11, e0168230.

689 Kuah, M.-K., Jaya-Ram, A., Shu-Chien, A.C., 2015. The capacity for long-chain
690 polyunsaturated fatty acid synthesis in a carnivorous vertebrate: Functional
691 characterisation and nutritional regulation of a Fads2 fatty acyl desaturase with Δ4
692 activity and an Elovl5 elongase in striped snakehead (*Channa striata*). Biochim.
693 Biophys. Acta - Mol. Cell Biol. Lipids 1851, 248-260.

694 Lee, J., Lee, H., Kang, S., Park, W., 2016. Fatty acid desaturases, polyunsaturated fatty
695 acid regulation, and biotechnological advances. Nutrients 8, 23.

696 Letunic, I., Bork, P., 2016. Interactive tree of life (iTOL) v3: an online tool for the display
697 and annotation of phylogenetic and other trees. Nucleic Acids Res. 44, W242-W245.

698 Li, Y., Monroig, Ó., Zhang, L., Wang, S., Zheng, X., Dick, J.R., You, C., Tocher, D.R.,
699 2010. Vertebrate fatty acyl desaturase with Δ4 activity. Proc. Natl. Acad. Sci. U. S.
700 A. 107, 16840-16845.

701 Linares, F., and Henderson, R. J. 1991. Incorporation of ^{14}C-labelled polyunsaturated
702 fatty acids by juvenile turbot, *Scophthalmus maximus* (L.) in vivo. J. Fish Biol. 38,
703 335-347.

704 Lowry, O.H., Rosebrough, N.J., Farr, A.L., Randall, R.J., 1951. Protein measurement
705 with the Folin phenol reagent. J. Biol. Chem. 193, 265-275.

706 Monroig, Ó., Li, Y., Tocher, D.R., 2011a. Delta-8 desaturation activity varies among fatty
707 acyl desaturases of teleost fish: High activity in delta-6 desaturases of marine
708 species. Comp. Biochem. Physiol. Part B Biochem. Mol. Biol. 159, 206-213.

709 Monroig, Ó., Lopes-Marques, M., Navarro, J. C., Hontoria, F., Ruivo, R., Santos, M.
710 M., Venkatesh, B., Tocher, D.R., Castro, L.F.C., 2016. Evolutionary functional
711 elaboration of the Elovl2/5 gene family in chordates. Sci. Rep. 6, 1-10.

712 Monroig, Ó., Tocher, D.R., Castro, L.F.C., 2018. Polyunsaturated fatty acid biosynthesis
713 and metabolism in fish, in: Burdge, G. (Ed.), Polyunsaturated Fatty Acid
714 Metabolism. AOCS Press, London, pp. 31-60.

715 Monroig, Ó., Wang, S., Zhang, L., You, C., Tocher, D.R., Li, Y., 2012. Elongation of
716 long-chain fatty acids in rabbitfish *Siganus canaliculatus*: Cloning, functional
717 characterisation and tissue distribution of Elovl5- and Elovl4-like elongases.
718 Aquaculture 350–353, 63-70.

719 Monroig, Ó., Webb, K., Ibarra-Castro, L., Holt, G.J., Tocher, D.R., 2011b. Biosynthesis

720 of long-chain polyunsaturated fatty acids in marine fish: Characterization of an
721 Elovl4-like elongase from cobia *Rachycentron canadum* and activation of the
722 pathway during early life stages. Aquaculture 312, 145-153.

723 Morais, S., Castanheira, F., Martinez-Rubio, L., Conceição, L.E.C., Tocher, D.R., 2012.
724 Long chain polyunsaturated fatty acid synthesis in a marine vertebrate: Ontogenetic
725 and nutritional regulation of a fatty acyl desaturase with Δ4 activity. Biochim.
726 Biophys. Acta - Mol. Cell Biol. Lipids 1821, 660-671.

727 Morais, S., Mourente, G., Martínez, A., Gras, N., Tocher, D.R., 2015. Docosahexaenoic
728 acid biosynthesis via fatty acyl elongase and Δ4-desaturase and its modulation by
729 dietary lipid level and fatty acid composition in a marine vertebrate. Biochim.
730 Biophys. Acta - Mol. Cell Biol. Lipids 1851, 588-597.

731 Mourente, G., Dick, J. R., Bell, J. G., Tocher, D. R. 2005. Effect of partial substitution of
732 dietary fish oil by vegetable oils on desaturation and β-oxidation of [1-^{14}C] 18: 3n-3
733 (LNA) and [1-^{14}C] 20: 5n-3 (EPA) in hepatocytes and enterocytes of European sea
734 bass (*Dicentrarchus labrax* L.). Aquaculture 248, 173-186.

735 Mourente, G., Tocher, D.R., 1993a. Incorporation and metabolism of ^{14}C-labelled
736 polyunsaturated fatty acids in juvenile gilthead sea bream *Sparus aurata* L. in vivo.
737 Fish Physiol. Biochem. 10, 443-453.

738 Mourente, G., Tocher, D.R., 1993b. Incorporation and metabolism of ^{14}C-labelled
739 polyunsaturated fatty acids in wild-caught juveniles of golden grey mullet, *Liza*
740 *aurata*, in vivo. Fish Physiol. Biochem. 12, 119-130.

741 Mourente, G., Tocher, D. R. 1994. In vivo metabolism of [1-^{14}C] linolenic acid (18: 3 (n−
742 3)) and [1-^{14}C] eicosapentaenoic acid (20: 5 (n− 3)) in a marine fish: Time-course of
743 the desaturation/elongation pathway. Biochim. Biophys. Acta, Lipids Lipid

744 Metab. 1212, 109-118.

745 Oboh, A., Kabeya, N., Carmona-Antoñanzas, G., Castro, L.F.C., Dick, J.R., Tocher, D.R.,
746 Monroig, Ó., 2017. Two alternative pathways for docosahexaenoic acid (DHA,
747 22:6n-3) biosynthesis are widespread among teleost fish. Sci. Rep. 7, 3889.

748 Pérez, J. A., Rodríguez, C., Bolaños, A., Cejas, J.R., Lorenzo, A., 2014. Beef tallow as
749 an alternative to fish oil in diets for gilthead sea bream (*Sparus aurata*) juveniles:
750 Effects on fish performance, tissue fatty acid composition, health and flesh
751 nutritional value. Eur. J. Lipid Sci. Technol. 116, 571-583.

752 Pérez, J. A., Rodríguez, C., Henderson, R. J. 1999. The uptake and esterification of
753 radiolabelled fatty acids by enterocytes isolated from rainbow trout (*Oncorhynchus*
754 *mykiss*). Fish Physiol. Biochem. 20, 125-134.

755 Rodríguez, C., Pérez, J.A., Henderson, R.J., 2002. The esterification and modification of
756 n-3 and n-6 polyunsaturated fatty acids by hepatocytes and liver microsomes of
757 turbot (*Scophthalmus maximus*). Comp. Biochem. Physiol. Part B Biochem. Mol.
758 Biol. 132, 559-570.

759 Ruyter, B., Sissener, N. H., Østbye, T. K., Simon, C. J., Krasnov, A., Bou, M., Sanden,
760 M., Nichols, P. D., Lutfi, E., Berge, G. M. 2019. n-3 Canola oil effectively replaces
761 fish oil as a new safe dietary source of DHA in feed for juvenile Atlantic
762 salmon. British Journal of Nutrition, 122, 1329-1345.

763 Sprague, M., Dick, J.R., Tocher, D.R., 2016. Impact of sustainable feeds on omega-3
764 long-chain fatty acid levels in farmed Atlantic salmon, 2006–2015. Sci. Rep. 6,
765 21892.

766 Sprecher, H., 2000. Metabolism of highly unsaturated n-3 and n-6 fatty acids. Biochim.
767 Biophys. Acta - Mol. Cell Biol. Lipids 1486, 219-231.

768 Tocher, D.R., 2015. Omega-3 long-chain polyunsaturated fatty acids and aquaculture in
769 perspective. Aquaculture 449, 94-107.

770 Tocher, D. R., Betancor, M. B., Sprague, M., Olsen, R. E., Napier, J. A. 2019. Omega-3
771 long-chain polyunsaturated fatty acids, EPA and DHA: bridging the gap between
772 supply and demand. Nutrients, 11, 89.

773 Tocher, D.R., Ghioni, C., 1999. Fatty acid metabolism in marine fish: Low activity of
774 fatty acyl Δ5 desaturation in gilthead sea bream (*Sparus aurata*) cells. Lipids 34,
775 433-440.

776 Trushenski, J. T., Rombenso, A. N., 2019. Trophic levels predict the nutritional
777 essentiality of polyunsaturated fatty acids in fish-introduction to a special section
778 and a brief synthesis. N Am J Aquacult, doi: 10.1 002/naaq.10137.

779 Vandesompele, J., De Preter, K., Pattyn, F., Poppe, B., Van Roy, N., De Paepe, A.,
780 Speleman, F., 2002. Accurate normalization of real-time quantitative RT-PCR data
781 by geometric averaging of multiple internal control genes. Genome Biol. 3(7),
782 research 0034.

783 Wilson, R., Sargent, J.R., 1992. High-resolution separation of polyunsaturated fatty acids
784 by argentation thin-layer chromatography. J. Chromatog. A, 623, 403-407.

785 Zar, J.H., 1999. Biostatistical Analysis, 4th ed. Prentice-Hall Inc., Upper Saddle River.

786 Zárate, R., el Jaber-Vazdekis, N., Tejera, N., Pérez, J.A., Rodríguez, C., 2017.
787 Significance of long chain polyunsaturated fatty acids in human health. Clin. Transl.
788 Med. 6, 25.

789 Zheng, X., Ding, Z., Xu, Y., Monroig, Ó., Morais, S., Tocher, D. R. 2009a. Physiological
790 roles of fatty acyl desaturases and elongases in marine fish: characterisation of
791 cDNAs of fatty acyl Δ6 desaturase and elovl5 elongase of cobia (*Rachycentron*

792 *canadum*). Aquaculture, 290, 122-131.

793 Zheng, X., Leaver, M.J., Tocher, D.R., 2009b. Long-chain polyunsaturated fatty acid
794 synthesis in fish: Comparative analysis of Atlantic salmon (*Salmo salar* L.) and
795 Atlantic cod (*Gadus morhua* L.) Δ6 fatty acyl desaturase gene promoters. Comp.
796 Biochem. Physiol. Part B Biochem. Mol. Biol. 154, 255-263.

Table 1. Sequences of primer pairs used in the cloning of *Sarpa salpa*, *Pegusa lascaris*, and *Chelon labrosus* fatty acyl elongase (*elovl5*) open reading frame (ORF) and for quantitative real-time PCR (qPCR) analysis of gene expression in tissues. Restriction sites *Bam*HI/*Xho*I for *S. salpa* (SSElovl5VF/SSElovl5VR), *P. lascaris* (PLElovl5VF/PLElovl5VR) and *C. labrosus* (CLElovl5VF/CLElovl5VR) are underlined in the corresponding primer sequences.

Aim	Species	Transcript	Primers	Primers sequence
First Fragment	*S. salpa*	*elovl5*	FFElovl5F1	5'- TACCCDCCAACCTTTGCACT -3'
			FFElovl5R1	5'- TCAATCCACCCTCAGCTTCTTG -3'
	P. lascaris		FFElovl5F1	5'- TACCCDCCAACCTTTGCACT -3'
			FFElovl5R2	5'- TCAATCCACCCTYAGYTTCTTG -3'
	C. labrosus		FFElovl5F1	5'- TACCCDCCAACCTTTGCACT -3'
			FFElovl5R2	5'- TCAATCCACCCTYAGYTTCTTG -3'
RACE PCR	*S. salpa*	*elovl5*	3'SSElovl5F1	5'- CCGTACCTTTGGTGGAAGAAGT -3'
			3'SSElovl5F2	5'- CAGTTCCAGCTGATCCAGTTCT -3'
			5'SSElovl5R1	5'- TTCATGTACTTGGGCCCCATC -3'
			5'SSElovl5R2	5'- GGTGGGTAGTTGTCGAGCAG -3'
	P. lascaris		3'PLElovl5F1	5'- CCCCATGCGATGGCTATACTT -3'
			3'PLElovl5F2	5'- ACGTACAAGAAGCGCAGTGT -3'
			5'PLElovl5R1	5'- GTAGAAGTTGTAGCCCCCGTG -3'
			5'PLElovl5R2	5'- TGTAGAGCACCAGAAGGCCT -3'
	C. labrosus		3'CLElovl5F1	5'- ACATGTTCACACTCACCATCCT -3'
			3'CLElovl5F2	5'- TCAGACTTACAAAAAGCGCAGC -3'
			5'CLElovl5R1	5'- CTTCCTCTGCGCTGTGAGTG -3'

			5’CLElovl5R2	5’- TTGTAGCCACCATGCCACAC -3’
ORF cloning	*S. salpa*	*elovl5*	SSElovl5UF	5’-CTCTCCCCTCCTCGAAAAGGTG -3’
			SSElovl5UR	5’-GAGAATGGGGTGACGGTTTCTCAAATG-3’
			SSElovl5VF	5’-CCCGGATCCAAAATGGAGACCTTC-3’
			SSElovl5VR	5’-CCGCTCGAGTCAATCCACTCTCAG-3’
	P. lascaris	*elovl5*	PLElovl5UF	5’-GTGTGTGTAATCGCTGATCTTCATGG-3’
			PLElovl5UR	5’-GATGTTGGGTGATACTTCCTCAAAGG-3’
			PLElovl5VF	5’-CCCGGATCCAAAATGGAGACCTTC-3’
			PLElovl5VR	5’-CCGCTCGAGTCAATCCACCCTTAG-3’
	C. labrosus	*elovl5*	CLElovl5UF	5’-GGCTGGGCGACTTGATGGTG-3’
			CLElovl5UR	5’-CCTCCTAGCAGCATTAGCTAACAC-3’
			CLElovl5VF	5’-CCCGGATCCAAAATGGAGGCCTTC-3’
			CLElovl5VR	5’- CCGCTCGAGTCAATCCACCCTC-3’
qPCR	*S. salpa*	*elovl5*	SSElovl5qF1	5’-ACAAGCACAGTGCGTCTCTAA-3’
			SSElovl5qR1	5’-ACGCACTACAGTGAGAATGGG-3’
	P. lascaris		PLElovl5qF1	5’-GCTGACAAAACCTGGAGAGC-3’
			PLElovl5qR1	5’-CCTCCTGGATGTCTTTTGGA-3’
	C. labrosus		CLElovl5qF1	5’-AGAACGGCTCCTCCCTATCA-3’
			CLElovl5qR1	5’-CAGCATTAGCTAACACGCTACA-3’
	S. salpa	*β-actin*	β-*actin*qF1	5’-CAGGGAGAAGATGACCCAGA-3’
			β-*actin*qR1	5’-ACAGTGCCCATCTATGAGGG-3’
	P. lascaris		β-*actin*qF1	5’-CAGGGAGAAGATGACCCAGA-3’
			β-*actin*qR1	5’-ACAGTGCCCATCTATGAGGG-3’
	C. labrosus		β-*actin*qF1	5’-CAGGGAGAAGATGACCCAGA-3’
			β-*actin*qR2	5’-CCCTCGTAGATGGGCACTGT-3’
	S. salpa	*elf1α*	*efl1α*qF1	5’-ATGCACCACGAGTCTCTGAC-3’
			*efl1α*qR1	5’-GGGTGGTTCAGGATGATGAC-3’

P. lascaris	*efl1α*qF2	5’-GTGGAGATGCACCACGAGTC-3’
	*efl1α*qR1	5’-GGGTGGTTCAGGATGATGAC-3’
C. labrosus	*efl1α*qF3	5’-GTCGAGATGCACCACGAGTC-3’
	*efl1α*qR1	5’-GGGTGGTTCAGGATGATGAC-3’

801 **Table 2.** Reaction conditions for cloning, functional characterization and gene expression of *elovl5* in *Sarpa salpa*, *Pegusa lascaris* and *Chelon*

802 *labrosus.*

Aim	Species	Transcript	Forward primer	Reverse primer	Denaturing temperature (°C) (duration in s)	Annealing temperature (°C) (duration in s)	Extension temperature (°C) (duration in s)	Number of cycles
First Fragment	*S. salpa*	*elovl5*	FFElovl5F1	FFElovl5R1	95 (30)	56 (45)	72 (60)	35
	P. lascaris		FFElovl5F1	FFElovl5R2	“	“	“	“
	C. labrosus		FFElovl5F1	FFElovl5R2	“	“	“	“
RACE PCR	*S. salpa*	*elovl5*	5' RACE Outer	5’SSElovl5R1	95 (30)	57 (30)	72 (90)	35
			5' RACE Inner	5’SSElovl5R2	“	“	“	“
			3’SSElovl5F1	3' RACE Outer	“	“	“	“
			3’SSElovl5F2	3' RACE Inner	“	“	“	“
	P. lascaris		5' RACE Outer	5’PLElovl5R1	95 (30)	57 (30)	72 (90)	35
			5' RACE Inner	5’PLElovl5R2	“	“	“	“
			3’PLElovl5F1	3' RACE Outer	“	“	“	“
			3’PLElovl5F2	3' RACE Inner	“	“	“	“
	C. labrosus		5' RACE Outer	5’CLElovl5R1	“	“	“	“
			5' RACE Inner	5’CLElovl5R2	“	“	“	“

			3’CLElovl5F1	3' RACE Outer	“	“	“	“
			3’CLElovl5F2	3' RACE Inner	“	59 (30)	“	“
ORF cloning	*S. salpa*	*elovl5*	SSElovl5UF	SSElovl5UR	95 (20)	55 (20)	72 (105)	40
			SSElovl5VF	SSElovl5VR	“	“	“	“
	P. lascaris	*elovl5*	PLElovl5UF	PLElovl5UR	95 (20)	55 (20)	72 (105)	35
			PLElovl5VF	PLElovl5VR	“	“	“	“
	C. labrosus	*elovl5*	CLElovl5UF	CLElovl5UR	95 (20)	55 (20)	72 (105)	40
			CLElovl5VF	CLElovl5VR	“	“	“	“
qPCR	*S. salpa*	*elovl5*	SSElovl5qF1	SSElovl5qR1	95 (15)	58.5 (30)	72 (30)	35
	P. lascaris		PLElovl5qF1	PLElovl5qR1	“	“	“	“
	C. labrosus		CLElovl5qF1	CLElovl5qR1	“	“	“	“
	S. salpa	*β-actin*	β-*actin*qF1	β-*actin*qR1	“	“	“	“
	P. lascaris		β-*actin*qF1	β-*actin*qR1	“	“	“	“
	C. labrosus		β-*actin*qF1	β-*actin*qR2	“	“	“	“
	S. salpa	*elf1α*	*efl1α*qF1	*efl1α*qR1	“	“	“	“
	P. lascaris		*efl1α*qF2	*efl1α*qR1	“	“	“	“
	C. labrosus		*efl1α*qF3	*efl1α*qR1	“	“	“	“

803 **Table 3.** Total lipid (mg lipid/mg protein) and main fatty acid composition (% of total FA) of control enterocytes and hepatocytes from *Sarpa*

804 *salpa, Pegusa lascaris* and *Chelon labrosus*.

	Sarpa salpa		*Pegusa lascaris*		*Chelon labrosus*	
	Enterocytes	Hepatocytes	Enterocytes	Hepatocytes	Enterocytes	Hepatocytes
Total lipid	0.9 ± 0.2	3.0 ± 1.5	1.2 ± 0.0	1.8 ± 0.6	0.8 ± 0.2	2.2 ± 0.5
Total saturated[1]	29.3 ± 1.8	35.5 ± 1.3	37.3 ± 1.6	50.4 ± 8.2	36.7 ± 6.0	44.2 ± 2.0
14:0	0.8 ± 0.1	1.0 ± 0.1	1.4 ± 0.3	2.8 ± 1.1	1.4 ± 0.7	1.8 ± 0.3
16:0	17.0 ± 0.8	22.5 ± 1.6	19.0 ± 0.5	31.3 ± 6.8	16.1 ± 8.5	23.0 ± 2.6
18:0	11.4 ± 0.2	10.0 ± 1.0	13.9 ± 2.2	13.5 ± 2.8	14.3 ± 1.9	10.8 ± 0.9
Total monoenes[1]	13.7 ± 0.5	19.6 ± 4.9	24.6 ± 5.6	28.9 ± 9.8	16.3 ± 2.8	23.4 ± 6.9
16:1[2]	1.9 ± 0.4	3.3 ± 2.5	2.6 ± 0.7	6.2 ± 2.0	2.0 ± 0.5	5.3 ± 3.8
18:1[3]	10.2 ± 0.9	15.3 ± 3.6	19.9 ± 4.3	19.1 ± 6.1	13.1 ± 1.9	16.5 ± 3.0
20:1[3]	0.7 ± 0.2	nd	0.2 ± 0.3	0.9 ± 0.4	0.7 ± 0.4	1.2 ± 0.9
Total n-6 PUFA[1]	22.9 ± 0.6	15.1 ± 1.3	8.9 ± 0.4	6.6 ± 2.0	16.3 ± 3.3	10.0 ± 3.6
18:2	3.5 ± 1.2	3.7 ± 0.7	4.0 ± 0.9	4.9 ± 3.0	7.7 ± 3.5	6.8 ± 2.1
18:3	nd	0.1 ± 0.2	nd	nd	nd	nd
20:3	1.4 ± 0.1	0.7 ± 0.1	nd	nd	nd	nd
20:4	14.9 ± 0.3	8.9 ± 1.6	2.5 ± 1.0	1.4 ± 0.6	5.9 ±1.9	2.7 ± 1.4
22:5	0.7 ± 0.1	0.6 ± 0.1	1.2 ± 0.2	0.1 ± 0.2	1.2 ± 0.2	0.5 ± 0.1
Total n-3 PUFA[1]	25.2 ± 2.5	23.0 ± 4.1	23.7 ± 6.3	9.7 ± 4.9	26.7 ± 5.7	16.8 ± 6.1
18:3	0.9 ± 0.2	1.0 ± 0.2	0.6 ± 0.0	0.6 ± 0.0	1.2 ± 0.4	1.2 ± 0.2
20:5	15.1 ± 1.6	10.3 ± 2.4	3.4 ± 0.2	2.1 ± 1.2	4.6 ± 1.1	2.5 ± 1.1
22:5	5.8 ± 0.5	5.2 ± 1.4	3.5 ± 1.2	1.7 ± 1.1	1.9 ± 0.5	0.7 ± 0.3
22:6	2.8 ± 0.3	5.1 ± 1.5	16.0 ± 5.0	5.2 ± 2.6	18.4 ± 4.9	12.3 ± 4.8
n-3/n-6	1.1 ± 0.1	1.5 ± 0.2	2.7 ± 0.6	1.7 ± 1.2	1.7 ± 0.6	1.7 ± 0.2
20:4n-6/20:5n-3	1.0 ± 0.1	0.9 ± 0.2	0.7 ± 0.3	0.7 ± 0.2	1.3 ± 0.3	1.0 ± 0.2
22:6n-3/20:5n-3	0.2 ± 0.0	0.5 ± 0.2	4.7 ± 1.7	2.7 ± 0.4	4.1 ± 1.0	5.1 ± 1.2
Total n-3 LC-PUFA[1]	24.3 ± 2.6	21.5 ± 4.4	23.0 ± 6.0	9.0 ± 4.8	26.7 ± 5.7	15.6 ± 6.1

805 Results are presented as mean ± SD (*S. salpa*, n=5; *P. lascaris*, n=3; *C. labrosus*, n= 6). LC-PUFA, long chain polyunsaturated fatty acids (≥ C20

806 and ≥ 2 double bonds); nd, not detected.[1] Includes some minor components not shown; [2] Mainly n-7 isomer; [3] Mainly n-9 isomer.

807 **Table 4.** Incorporation of radioactivity into total lipids (pmol mg prot^{-1} h^{-1}) of isolated enterocytes and hepatocytes of *Sarpa salpa*, *Pegusa*

808 *lascaris* and *Chelon labrosus* incubated with [1-^{14}C] 18:2n-6, [1-^{14}C] 18:3n-3, [1-^{14}C] 20:5n-3 and [1-^{14}C] 22:6n-3.

	ENTEROCYTES				HEPATOCYTES			
[1-^{14}C] FA	18:2n-6	18:3n-3	20:5n-3	22:6n-3	18:2n-6	18:3n-3	20:5n-3	22:6n-3
Species								
Sarpa salpa	90.5 ± 26.7 ^{c}	75.6 ± 26.0 ^{bc}	38.6 ± 19.7 ^{ab}	25.2 ± 10.7 ^{a}	154.7 ± 49.3	100.4 ± 37.9	71.2 ± 40.1	85.0 ± 49.5
Pegusa lascaris	471.4 ± 50.9 ^{c}	211.9 ± 7.3 ^{b}	127.6 ± 45.6 ^{b}	59.7 ± 19.8 ^{a}	142.2 ± 18.4 ^{b}	173.0 ± 12.5 ^{b}	54.3 ± 31.5 ^{a}	58.2 ± 4.9 ^{a}
Chelon labrosus	67.0 ± 16.3 ^{b}	67.5 ± 19.8 ^{b}	32.7 ± 13.8 ^{a}	12.3 ± 3.1 ^{a}	57.3 ± 35.3 ^{b}	88.5 ± 58.6 ^{b}	51.1 ± 25.4 ^{b}	10.7 ± 6.1 ^{a}

809 Values are presented as mean ± SD (*S. salpa*, n=5, except for [1-^{14}C] 22:6n-3, where n=4; *P. lascaris*, n=3; *C. labrosus*, n= 6). Different letters in

810 superscript denote significant differences between [1-^{14}C] FA for each cell type ($p<0.05$).

811 **Table 5.** Bioconversions (% of total radioactivity) registered in isolated enterocytes and
812 hepatocytes from *Sarpa salpa*, *Pegusa lascaris* and *Chelon labrosus* incubated with [1-
813 ^{14}C] 18:2n-6, [1-^{14}C] 18:3n-3 and [1-^{14}C] 20:5n-3.

	Sarpa salpa					
	ENTEROCYTES			HEPATOCYTES		
[1-^{14}C] PUFA	18:2	18:3	20:5	18:2	18:3	20:5
FA recovery	85.0 ± 5.0 ^{b}	89.4 ± 3.5 ^{b}	63.0 ± 2.8 ^{a}	80.8 ± 6.1 ^{b}	84.4 ± 2.0 ^{b}	68.0 ± 2.5 ^{a}
Elongation	10.5 ± 5.3 ^{a}	8.1 ± 4.0 ^{a}	20.8 ± 3.3 ^{b}	8.7 ± 3.8 ^{a}	9.7 ± 3.5 ^{a}	17.4 ± 1.7 ^{b}
Desaturation	nd	0.3 ± 0.4	nd	1.7 ± 0.4	2.3 ± 1.0	nd
E+D	2.4 ± 1.4 ^{ab}	0.5 ± 0.7 ^{a}	2.8 ± 1.2 ^{b}	7.0 ± 2.5 ^{b}	3.5 ± 1.8 ^{a}	1.9 ± 0.8 ^{a}
De novo	1.9 ± 0.2 ^{a}	1.2 ± 0.6 ^{a}	12.8 ± 3.9 ^{b}	1.2 ± 0.2 ^{a}	nd	10.0 ± 3.8 ^{b}
Unknown	0.2 ± 0.2	0.5 ± 0.2	0.5 ± 1.1	0.6 ± 0.8	nd	2.6 ± 1.9
	Pegusa lascaris					
	ENTEROCYTES			HEPATOCYES		
[1-^{14}C] PUFA	18:2	18:3	20:5	18:2	18:3	20:5
FA recovery	87.0 ± 1.8 ^{b}	92.3 ± 3.1 ^{b}	70.7 ± 5.1 ^{a}	80.6 ± 5.0 ^{b}	89.3 ± 3.2 ^{b}	59.1 ± 8.6 ^{a}
Elongation	9.6 ± 0.9 ^{a}	6.8 ± 2.7 ^{a}	21.1 ± 1.0 ^{b}	13.3 ± 3.4 ^{a}	8.1 ± 4.2 ^{a}	32.1 ± 7.2 ^{b}
Desaturation	1.0 ± 0.7	nd	nd	2.0 ± 0.7	nd	nd
E+D	2.2 ± 0.6	0.8 ± 0.7	4.6 ± 5.9	3.5 ± 1.1 ^{b}	1.6 ± 0.5 ^{a}	2.7 ± 0.3 ^{ab}
De novo	nd	nd	3.6 ± 4.5	nd	1.0 ± 1.7	6.1 ± 3.7
Unknown	0.2 ± 0.1	0.1 ± 0.2	nd	0.5 ± 1.0	nd	nd
	Chelon labrosus					
	ENTEROCYTES			HEPATOCYTES		
[1-^{14}C] PUFA	18:2	18:3	20:5	18:2	18:3	20:5
FA recovery	83.9 ± 2.8 ^{b}	89.7 ± 0.6 ^{c}	62.4 ± 2.0 ^{a}	66.4 ±14.4 ^{a}	92.2 ± 1.6 ^{b}	77.5 ± 4.3 ^{a}
Elongation	4.0 ± 1.0 ^{a}	4.5 ± 1.2 ^{a}	28.4 ± 1.2 ^{b}	9.5 ± 9.4 ^{ab}	2.0 ± 1.9 ^{a}	21.9 ± 3.4 ^{b}
Desaturation	nd	nd	nd	nd	nd	nd
E+D	5.4 ± 0.9 ^{b}	3.5 ± 0.9 ^{a}	nd	22.2 ±13.8	5.5 ± 1.6	nd
De novo	5.6 ± 0.7 ^{b}	nd	0.3 ± 0.4 ^{a}	1.8 ± 2.8	0.3 ± 0.6	nd
Unknown	1.1 ± 1.2	2.3 ± 0.5	8.9 ± 2.2	nd	nd	0.6 ± 1.0

814 Values are presented as mean ± SD (*S. salpa*, n=5; *P. lascaris*, n=3; *C. labrosus*, n= 6).
815 E+D, elongation and desaturation; nd, not detected. *De novo*: shorter FAs produced by
816 using the [1-^{14}C] released after a first β-oxidation cycle of the radiolabeled substrate.
817 Different letters in superscript denote significant differences between [1-^{14}C] fatty acids
818 for each cell type ($p<0.05$).

819 **Table 6.** Products obtained (% of total radioactivity) from the incubation of isolated

820 enterocytes and hepatocytes with [1-^{14}C] 18:2n-6, [1-^{14}C] 18:3n-3 and [1-^{14}C] 20:5n-3

	ENTEROCYTES			HEPATOCYTES		
	S. salpa	*P. lascaris*	*C. labrosus*	*S. salpa*	*P. lascaris*	*C. labrosus*
[1-^{14}C]18:2n-6						
18:3	nd	1.0 ± 0.7	nd	1.7 ± 0.4	2.0 ± 0.7	nd
20:2	8.0 ± 5.2	8.3 ± 1.2	2.0 ± 0.5	7.2 ± 3.4	12.2 ± 0.8	4.4 ± 4.2
20:3	nd	0.4 ± 0.3	nd	0.9 ± 0.9	0.3 ± 0.5	nd
20:4	nd	nd	1.3 ± 0.4	0.4 ± 0.5	nd	9.9 ± 6.7
22:2	2.6 ± 0.8	1.3 ± 0.9	1.9 ± 0.6	1.5 ± 1.0	1.1 ± 1.9	5.1 ± 5.2
22:4	1.2 ± 0.3	nd	0.8 ± 0.4	1.2 ± 1.2	nd	nd
22:5	1.3 ± 1.1	1.5 ± 1.0	3.3 ± 0.5	4.6 ±1.9	3.2 ± 1.1	12.3± 7.2
24:5	nd	0.3 ± 0.6	nd	nd	nd	nd
[1-^{14}C]18:3n-3						
18:4	0.3 ± 0.4	nd	nd	2.3 ± 1.0	nd	nd
20:3	7.2 ± 3.5	6.5 ± 2.9	1.5 ± 0.4	8.8 ± 4.0	8.1 ± 4.2	2.0 ± 1.9
20:4	nd	nd	1.5 ± 0.4	1.0 ± 0.3	nd	3.3 ± 3.2
20:5	nd	0.3 ± 0.2	0.8 ± 0.3	nd	1.2 ± 0.4	0.8 ± 0.7
22:3	1.0 ± 0.9	0.2 ± 0.4	0.9 ± 0.5	0.9 ± 0.9	nd	nd
22:5	nd	nd	0.1 ± 0.2	0.4 ± 0.4	nd	nd
22:6	nd	0.5 ± 0.5	1.2 ± 0.3	0.9 ± 0.3	0.4 ± 0.7	1.4 ± 1.2
24:3	nd	nd	0.9 ± 0.5	nd	nd	nd
24:6	0.5 ± 0.7	nd	nd	1.2 ± 1.1	nd	nd
[1-^{14}C]20:5n-3						
22:5	15.3 ± 2.6	12.7 ± 1.7	15.0 ± 0.3	14.6 ± 1.2	23.3 ± 4.4	12.4 ± 3.5
22:6	nd	4.6 ± 5.9	nd	nd	2.7 ± 0.3	nd
24:5	5.6 ± 2.1	8.4 ± 2.6	4.1 ± 0.7	2.8 ± 0.8	8.7 ± 4.3	4.9 ± 2.9
24:6	2.8 ± 1.2	nd	nd	1.9 ± 0.8	nd	nd

821 Values are presented as mean ± SD (*S. salpa*, n=5; *P. lascaris*, n=3; *C. labrosus*, n= 6).

822 nd, not detected.

823 **Table 7**. Percentage of conversion of fatty acid (FA) substrates exogenously added to
824 transgenic yeast (*Saccharomyces cerevisiae*) transformed with the coding region of *elovl5*
825 from *Sarpa salpa, Pegusa lascaris* and *Chelon labrosus*.

		% conversion		
FA substrate	FA product	*Sarpa salpa*	*Pegusa lascaris*	*Chelon labrosus*
18:2n-6	20:2n-6	5.1	29.6	15.2
18:3n-3	20:3n-3	29.3	44.7	42.0
18:3n-6	20:3n-6	38.3	81.6	58.4
18:4n-3	20:4n-3	50.2	80.3	64.4
20:4n-6	22:4n-6	30.2	36.1	27.0
20:5n-3	22:5n-3	75.7	70.8	69.1
22:4n-6	24:4n-6	nd	nd	nd
22:5n-3	24:5n-3	nd	2.3	nd

826 Results are expressed as a percentage of total fatty acid substrate converted to elongated
827 product. nd, not detected.

828 **Table SD (Supplementary data).** Total lipid (% wet weight) and main fatty acid
829 composition (% of total FA) of muscle from *Sarpa salpa*, *Pegusa lascaris* and *Chelon*
830 *labrosus*.

	Sarpa salpa	*Pegusa lascaris*	*Chelon labrosus*
Total lipid	0.5 ± 0.1	0.5 ± 0.1	0.9 ± 0.1
Total saturated[1]	27.1 ± 0.7	28.8 ± 1.0	32.8 ± 2.2
14:0	0.8 ± 0.1	1.0 ± 0.5	2.7 ± 0.6
16:0	18.6 ± 0.5	18.2 ± 1.0	23.1 ± 1.7
18:0	6.4 ± 0.3	7.4 ± 0.4	5.8 ± 1.0
Total monoenes[1]	20.9 ± 2.4	17.9 ± 1.9	24.0 ± 3.2
16:1[2]	2.9 ± 0.5	2.7 ± 1.0	6.6 ± 1.1
18:1[3]	17.3 ± 2.1	13.6 ± 0.6	16.7 ± 2.5
20:1[3]	0.0 ± 0.1	0.6 ± 0.5	0.4 ± 0.1
Total n-6 PUFA[1]	19.1 ± 0.6	8.2 ± 0.9	16.8 ± 1.1
18:2	5.4 ± 1.7	1.4 ± 0.3	10.5 ± 1.9
18:3	0.4 ± 0.0	nd	0.4 ± 0.1
20:3	0.8 ± 0.0	nd	0.2 ± 0.2
20:4	10.7 ± 1.0	4.3 ± 0.7	3.9 ± 0.7
22:5	0.5 ± 0.2	1.3 ± 0.2	1.0 ± 0.3
Total n-3 PUFA[1]	28.4 ± 2.3	41.4 ± 2.4	23.0 ± 3.3
18:3	1.1 ± 0.2	0.4 ± 0.1	1.8 ± 0.5
20:5	16.9 ± 1.7	6.0 ± 0.3	7.0 ± 1.2
22:5	5.5 ± 0.6	5.9 ± 0.6	2.1 ± 0.4
22:6	3.6 ± 0.4	28.7 ± 2.9	10.4 ± 3.1
n-3/n-6	1.5 ± 0.2	5.1 ± 0.6	1.4 ± 0.2
20:4n-6/20:5n-3	0.6 ± 0.0	0.7 ± 0.2	0.6 ± 0.1
22:6n-3/20:5n-3	0.2 ± 0.0	4.8 ± 0.7	1.5 ± 0.6
Total n-3 LC-PUFA[1]	26.8 ± 2.3	40.6 ± 2.4	20.0 ± 3.0

831 Results are presented as mean ± SD (*S. salpa*, n=5; *P. lascaris*, n=7; *C. labrosus*, n= 6).
832 LC-PUFA, Long chain polyunsaturated fatty acids (≥ C20 and ≥ 2 double bonds); nd, not
833 detected.[1] Includes some minor components not shown; [2] Mainly n-7 isomer; [3] Mainly n-
834 9 isomer.

835 **Figure legend**

836 **Figure 1.** Long-chain (C20-24) polyunsaturated fatty acids biosynthetic route from
837 linoleic (n-6) and α-linolenic acid (n-3).

838 **Figure 2.** Phylogenetic tree of *elovl5* using the deduced amino acid sequences from *Sarpa*
839 *salpa*, *Pegusa lascaris* and *Chelon labrosus*. The number over horizontal branch length
840 shows the branch lengths which is proportional to the amino acid substitution rate per
841 site, whereas the percentage number under the horizontal branch length is the bootstrap
842 replicates from 1000 iterations.

843 **Figure 3.** Tissue distribution of *elovl5* in *Sarpa salpa*, *Pegusa lascaris* and *Chelon*
844 *labrosus*. Data are presented as geometric mean log normalized expression ratios ±
845 standard errors (*S. salpa* and *P. lascaris* n=4; *C. labrosus*, n=3). Different letters denote
846 significant differences among tissue for each specie ($p<0.05$).

847

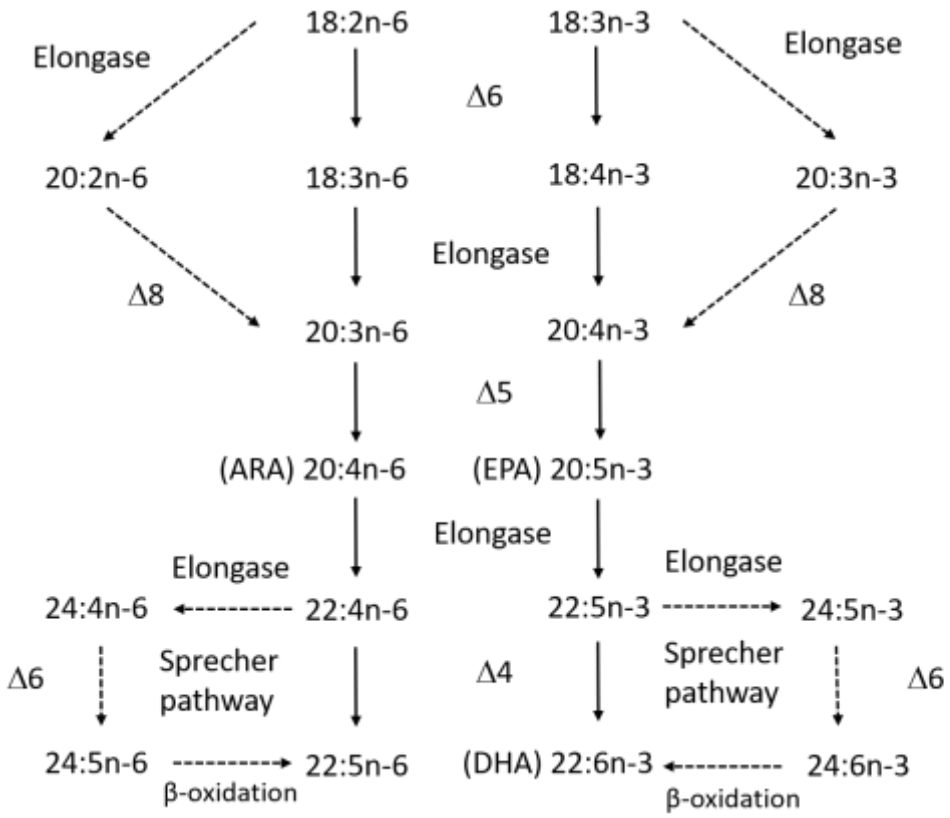
18:2n-6
18:3n-3
Elongase
Elongase
Δ6
20:2n-6
18:3n-6
18:4n-3
20:3n-3
Elongase
Δ8
Δ8
20:3n-6
20:4n-3
Δ5
(ARA) 20:4n-6
(EPA) 20:5n-3
Elongase
Elongase
Elongase
24:4n-6
22:4n-6
22:5n-3
24:5n-3
Δ6
Sprecher pathway
Δ4
Sprecher pathway
Δ6
24:5n-6
22:5n-6
(DHA) 22:6n-3
24:6n-3
β-oxidation
β-oxidation

848

849

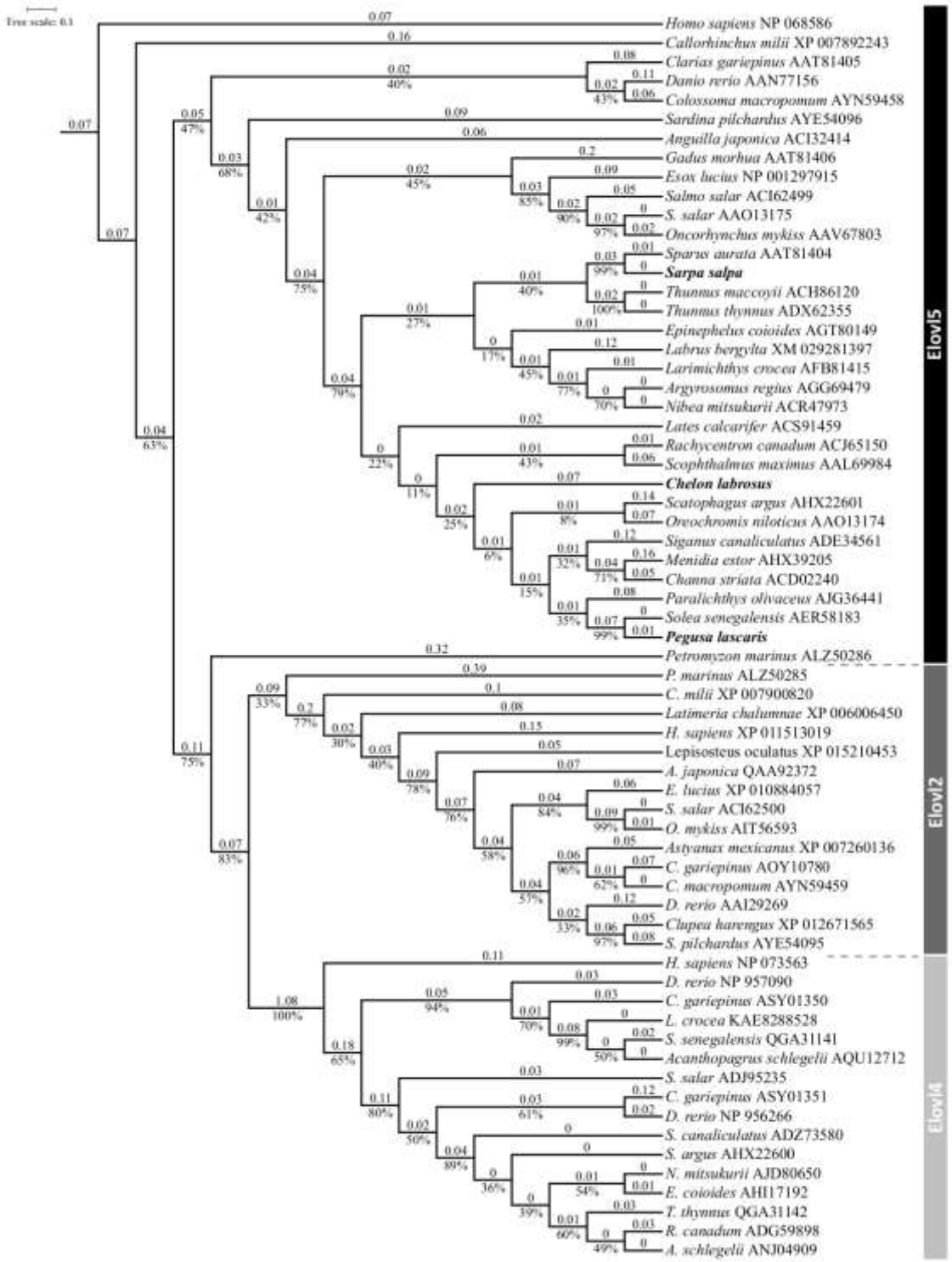
Tree scale: 0.1
Homo sapiens NP 068586
Callorhinchus milii XP 007892243
Clarias gariepinus AAT81405
Danio rerio AAN77156
Colossoma macropomum AYN59458
Sardina pilchardus AYE54096
Anguilla japonica ACI32414
Gadus morhua AAT81406
Esox lucius NP 001297915
Salmo salar ACI62499
S. salar AAO13175
Oncorhynchus mykiss AAV67803
Sparus aurata AAT81404
Sarpa salpa
Thunnus maccoyii ACH86120
Thunnus thynnus ADX62355
Epinephelus coioides AGT80149
Labrus bergylta XM 029281397
Larimichthys crocea AFB81415
Argyrosomus regius AGG69479
Nibea mitsukurii ACR47973
Lates calcarifer ACS91459
Rachycentron canadum ACJ65150
Scophthalmus maximus AAL69984
Chelon labrosus
Scatophagus argus AHX22601
Oreochromis niloticus AAO13174
Siganus canaliculatus ADE34561
Menidia estor AHX39205
Channa striata ACD02240
Paralichthys olivaceus AJG36441
Solea senegalensis AER58183
Pegusa lascaris
Petromyzon marinus ALZ50286
P. marinus ALZ50285
C. milii XP 007900820
Latimeria chalumnae XP 006006450
H. sapiens XP 011513019
Lepisosteus oculatus XP 015210453
A. japonica QAA92372
E. lucius XP 010884057
S. salar ACI62500
O. mykiss AIT56593
Astyanax mexicanus XP 007260136
C. gariepinus AOY10780
C. macropomum AYN59459
D. rerio AAI29269
Clupea harengus XP 012671565
S. pilchardus AYE54095
H. sapiens NP 073563
D. rerio NP 957090
C. gariepinus ASY01350
L. crocea KAE8288528
S. senegalensis QGA31141
Acanthopagrus schlegelii AQU12712
S. salar ADJ95235
C. gariepinus ASY01351
D. rerio NP 956266
S. canaliculatus ADZ73580
S. argus AHX22600
N. mitsukurii AJD80650
E. coioides AHI17192
T. thynnus QGA31142
R. canadum ADG59898
A. schlegelii ANJ04909
Elovl5
Elovl2
Elovl4

850

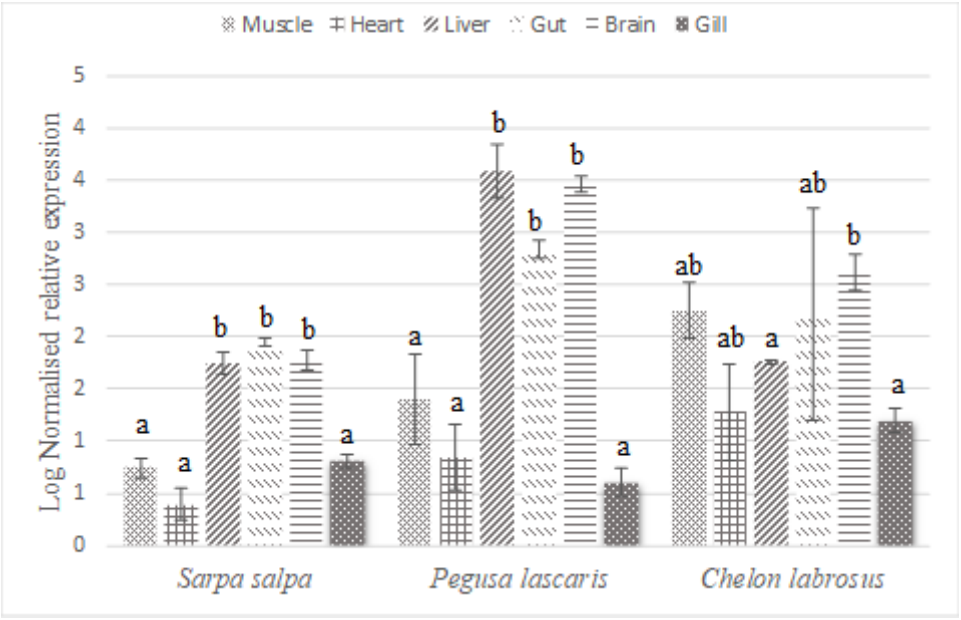
Muscle
Heart
Liver
Gut
Brain
Gill
Log Normalised relative expression
0
1
1
2
2
3
3
4
4
5
a
a
b
b
b
a
a
b
a
b
b
a
ab
ab
a
ab
b
a
Sarpa salpa
Pegusa lascaris
Chelon labrosus

851